CECIL AND IDA GREEN INSTITUTE OF GEOPHYSICS AND PLANETARY PHYSICS

2019 ANNUAL REPORT

SCRIPPS INSTITUTION OF OCEANOGRAPHY | UNIVERSITY OF CALIFORNIA, SAN DIEGO

IGPP 2019

DIRECTOR'S WELCOME

Here is the 2019 Annual Report of the Cecil and Ida Green Institute of Geophysics and Planetary Physics, in which we provide descriptions of our research activities carried out during the past year. This report, as well as its predecessors dating back to 2006, is designed to give prospective graduate students, and anyone else who is interested in geophysics, an overview of our research, which spans a broad range of subjects in geophysics, oceanography, geology, and, indeed, planetary science.

Much of our work could be described as pure science, but the subject matter is often of broad societal interest, such as understanding earthquake mechanisms and cycles, studying the behavior of ice sheets, improving methods for energy exploration (both renewable and conventional), monitoring carbon dioxide sequestration, the effects of drought on California groundwater, the effects of atmospheric water on storm systems, modeling Earth's magnetic field, and so on. A lot of what we do involves long-term monitoring of the sea, land, and atmosphere by operating and using a variety of instrument networks as well as shipboard systems. IGPP has a strong history of instrument development, but also the development of theoretical and numerical methods. We hope you find this report useful and agree that IGPP continues to be one of the leading research centers for geophysics.

Sadly, the founding Director of IGPP, Walter Munk, passed away this year at the age of 101. Walter was an intellectual giant, and his pioneering research into surf forecasting, swell propagation, ocean currents, tides, time series analysis, ocean acoustics, and ocean temperature will be remembered by many. Those of us who frequented the halls of IGPP will have a special memory of him, and his birthday, October 19, will be Walter Munk Day at IGPP, featuring a special lecture which was given this year by IGPP alumna Professor Catherine Johnson.

Steven Constable, Director, IGPP

Recovering a seafloor EM instrument off Alaska

CONTENTS

** Individual report not available this year*

GREEN FOUNDATION

The Cecil H. and Ida M. Green Foundation for Earth Sciences supports visiting scholars and resident scientists at IGPP. Established with a gift from the late Cecil Green in 1971, the Green Foundation holds an endowment managed by the UC San Diego-IGPP Director and overseen by an independent Board of Directors. A selection committee comprised of IGPP faculty screens nominees and applicants for both the Green Scholar and the Miles Fellowship.

The Green Foundation is currently supporting:

Green Scholar: *James Badro, IPGP, France*

Green Scholar: *Catherine Johnson, UBC, Canada*

Green Scholar: *Pieter-Ewald Share, postdoc*

Green Scholar: *Brook Tozer, postdoc*

Green Scholar: *Shunguo Wang, postdoc*

Miles Fellow: *Ignacio Sepulveda, postdoc*

UC San Diego membership in Southern California Earthquake Center *www.scec.org*

GRADUATE PROGRAM

More than the Oceans...

Our multidisciplinary program offers graduate students a unique hands-on, collaborative learning environment. In addition to our core academic curriculum, we emphasize observational techniques and the collection of novel datasets.

Graduate Students who successfully defended in 2019

Matthew Cook, Ph.D. *(Zumberge): Calibrated Ocean Bottom Pressure Measurements for Marine Geodesy*

Adrian Doran, Ph.D. *(Laske): Imaging Oceanic Crust with Broadband Seismic and Pressure Data*

Jessie Saunders, Ph.D. *(Hasse): A Multi-Sensor Approach to Identifying Shallow Slip for Near-Shore Tsunami Early Warning*

Wei Wang, Ph.D. *(Shearer): Attenuation and Scattering Structure of Southern California and Tidal Triggering of Earthquakes*

Yongfei Wang, Ph.D. *(Shearer): Dynamic Modeling of Pulse-like earthquake and ground motion*

Sandra Slead, MS *(Sandwell): Tracking Surface Deformation and Magma Storage at Okmok Volcano with InSAR and GPS*

WALTER MUNK 1917–2019

Obituary of IGPP's founding director by Peter F. Worcester (pworcester@ucsd.edu) and Robert C. Spindel (spindel@uw.edu) from Acoustics Today, *15(2), 62*

Walter H. Munk, an oceanographer and geophysicist who made seminal contributions to ocean acoustics, physical oceanography, and geophysics over a career spanning nearly 80 years, died at his home in La Jolla, CA, on February 8, 2019, at the age of 101.

Walter was born on October 19, 2017, in Vienna, Austria. He was sent to the United States at age 14 to finish high school. After an unhappy time at a financial firm in which his grandfather was a partner, he applied to Cal Tech, graduating in 1939 in Applied Physics. Walter first came to the Scripps Institution of Oceanography in 1939 for a summer job. He obtained a Master's Degree from Cal Tech in 1940 before returning to Scripps, where the Director, Harald Sverdrup, accepted him as a Ph.D. student.

Believing that war was imminent, Walter enlisted in the Army. He was discharged in December 1941, one week before Pearl Harbor, to join the University of California Division of War Research. During the war, Walter and Sverdrup developed a system to forecast wave conditions in preparation for the Allied landings in Africa. Their methods successfully predicted that the conditions for the D-Day landing in Normandy would be rough, but manageable. Walter received his Ph.D. in 1947. He spent his entire career at Scripps, founding and serving as Director of the La Jolla Laboratories of the Institute of Geophysics and Planetary Physics from 1962 to 1982.

Walter made contributions to so many fields that there are some who think that there is more than one Walter Munk. In the early 1950s, he made fundamental contributions to our understanding of the wind-driven ocean circulation, coining the term "ocean gyres." He then became interested in the irregularities in the earth's rotation (wobble and spin), which form an elegant remote sensing tool from which one can infer information about the Earth's core, its air and water masses, and global winds. He made pioneering measurements of ocean swell (1958–1968) and deep-sea tides (1964–1974). He was one of the initiators of 1962 Project MOHOLE to drill into the Earth's mantle. In the early 1970s, Walter and Christopher Garrett devised the Garrett-Munk formulation of the ocean internal wave spectrum. In the mid-1970s, he was lured into the world of ocean acoustics through his participation in JASON (a scientific advisory group to the Department of Defense), which at the time was working on anti-submarine warfare. He was among the first to realize that internal waves cause sound-speed fluctuations, leading to fluctuations in acoustic signals. He, together with Peter Worcester and Carl Wunsch, invented ocean acoustic tomography to study the ocean mesoscale. He subsequently proposed that acoustic transmissions be used to study ocean warming on global scales and led the 1991 Heard Island Feasibility Test (HIFT) in which transmissions from near Heard Island in the southern Indian Ocean were recorded on receivers in both the Pacific and Atlantic. HIFT was followed by the decade-long Acoustic Thermometry of Ocean Climate (ATOC) series of experiments in the North Pacific.

Walter has received every conceivable honor, from the National Medal of Science to the Kyoto Prize to the Crafoord Prize. He is an Honorary Fellow of the ASA. The United States Navy and The Oceanography Society established the Walter Munk Award for Distinguished Research in Oceanography Related to Sound in the Sea in his honor.

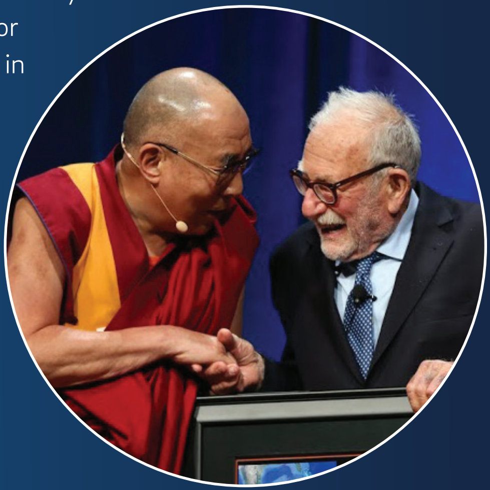

Munk is preceded in death by wife Judith, who died in 2006, and daughter Lucian, who was born with a heart defect and died at the age of 7 in 1961. He is survived by daughters Edie of La Jolla and Kendall of State College, PA, three grandsons Walter, Lucien, and Maxwell, and current spouse Mary Coakley Munk. A more complete account of Walter's life, including a list of selected publications, is available in Spindel, R. C., and Worcester, P. F. (2016). "Walter H. Munk: Seventy-Five Years of Exploring the Seas," *Acoustics Today* 12, 36–42.

Mw 6.4 and Mw 7.1 EQs SHIFT THE EARTH

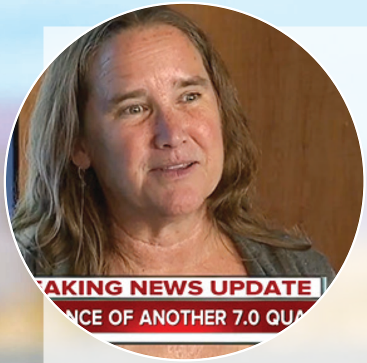

After the July 2019 Ridgecrest quakes rattled Southern California, IGPP researchers stood in front of news cameras to reassure the public and dove into the field to learn more about the new the state's newly revealed fault line.

The 4th of July had a bit more in store for Southern California than the usual fireworks and parades. A magnitude 6.4 quake shook a remote area in the state, the Naval Air Station China Lake, ~10 miles from the town of Ridgecrest. The event, while tremendous, was even more remarkably followed by a Mw 7.1 in the same area, about 36 hours later and felt as far away as Arizona and Mexico. The two quakes were determined to be neither foreshocks nor aftershocks, but a rare mainshock pair called an "Earthquake Doublet" according to IGPP seismologists Debi Kilb and Frank Vernon who were onsite to answer questions and allay public fears when regional news crews arrived.

Will this trigger the Big One? Though "we live in Earthquake Country," according to Kilb, the new fault is likely too far from the San Andreas Fault to for this doublet ruptures to have an impact on California's 800mile fault. Instead Kilb and Vernon monitored seismic activity of the Garlock Fault and Coso Volcanic Field, where more proximal aftershocks did occur.

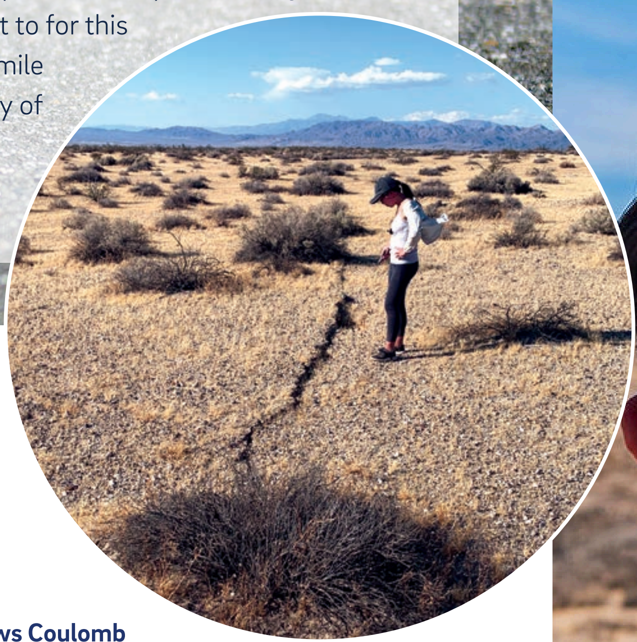

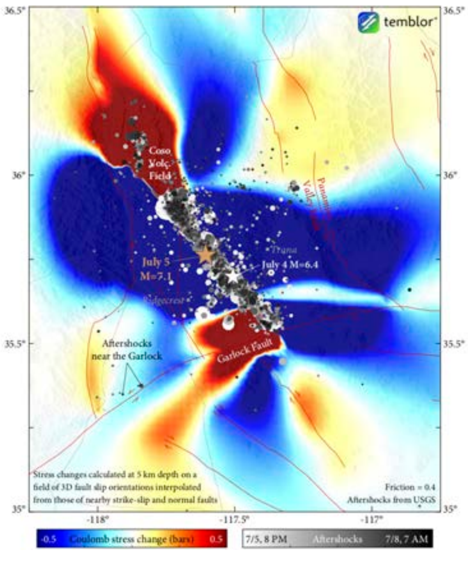

The graphic shows Coulomb stress changes imparted by the Mw 7.1 quake to faults that are optimally oriented for failure under the regional tectonic stress direction. Image courtesy of Debi Kilb, further explanation available at http://sumo.ly/13l92 via @temblor

IGPP researchers have been studying Ridgecrest Doublet since it occurred. The new fault offers an excellent proving ground to test sensor systems and examine tectonic stress direction.

SOPAC MEASURES COSEISMIC OFFSETS

Scripps Orbit and Permanent Array Center (SOPAC), led by Yehuda Bock, Peng Fang, Dorian Golriz quickly estimated coseismic offsets for the July 4 and July 5 earthquakes—the total displacements of GNSS stations within several hundred kilometers from the source were calculated, as well as the effect of each individual event. SOPAC found 98 stations with detectable signals (>3 mm). The closest station was offset by about 100 mm to the east during the July 4 event and about 580 mm to the SSE as a result of the July 5 event. As part of SOPAC's operational daily analysis, they identified another 66 stations with detectable signals as far away as the Los Angeles basin. SOPAC's coseismic offsets were used by **Xiaohua (Eric) Xu** in **David Sandwell's group** as input to static fault slip models and stress calculations for the two events to supplement the available InSAR images.

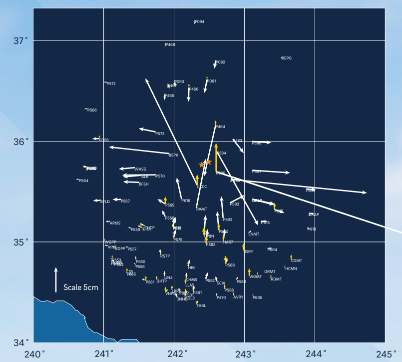

Total coseismic displacements for the M6.4 and M7.1 earthquakes on July 4 and 5, 2019.

SOPAC then analyzed the high-rate (5-10 Hz) GNSS data provided by UNAVCO to estimate displacement waveforms, useful as input to kinematic fault slip models and to further develop earthquake early warning systems for predicting S- and surface-wave arrivals and to rapidly estimate an earthquake's magnitude using peak ground displacements. These and seismic data were used by Dorian Golriz to bracket the coseismic time window for each station to be able to distinguish coseismic motions from early postseismic deformation. Golriz also used accelerometer and GNSS data to compute seismogeodetic velocity and displacements waveforms at collocated GNSS/seismic stations. This combination of GNSS and even low-cost MEMS accelerometers effectively provides broadband seismometer records, from the Nyquist frequency (typical 50 Hz) to the DC offsets, that do not clip near the source. Data and products from these studies as well as SOPAC's operational displacement time series with modeled coseismic and postseismic motions may be obtained from the SOPAC data archive at sopac-csrc.ucsd.edu.

CO-SEISMIC DISPLACEMENTS AND SURFACE FRACTURES

Xiaohua Xu and David T. Sandwell have applied Interferometric Synthetic Aperture Radar (InSAR), an important tool for imaging surface deformation from large continental earthquakes, to better understand displacement and strain from the 2019 Ridgecrest earthquakes. Xu and Sandwell developed maps to show co-seismic displacement and strain using multiple Sentinel-1 images. They provide three types of interferometric products. (1) Standard interferograms from two look directions provide an overview of the deformation and can be used for modeling co-seismic slip. (2) Phase gradient maps from stacks of co-seismic nterferograms provide high resolution (~30 m) images of strain concentration and surface fracturing that can be used to guide field surveys. (3) High-pass filtered, stacked, unwrapped phase is decomposed into east-west and up-down/south-north components and is used to determine the sense of fault slip. The phase gradient maps reveal over 300 surface fractures including triggered slip on the Garlock fault. The east-west component of high pass filtered phase reveals the polarity of the strike-slip offset (right-lateral or left-lateral) for many of the fractures. Xu and Sandwell found a small number of fractures that have slip polarity that is retrograde to the background tectonic stress. This is similar to observations of retrograde slip observed near the 1999 Mw 7.1 Hector Mine rupture but they are more completely imaged by the frequent and high-quality acquisitions from the twin Sentinel-1 spacecrafts.Determining whether the retrograde features are triggered slip on existing fault, or compliant fault deformation in response to stress from the earthquakes, or new Coulomb failures, will require additional field work, modeling, and analysis.

Read Further: X. Xu, D. T. Sandwell, B. Smith-Konter; Coseismic Displacements and Surface Fractures from Sentinel-1 InSAR: 2019 Ridgecrest Earthquakes. *Seismol. Res. Lett.* doi.org/10.1785/0220190275

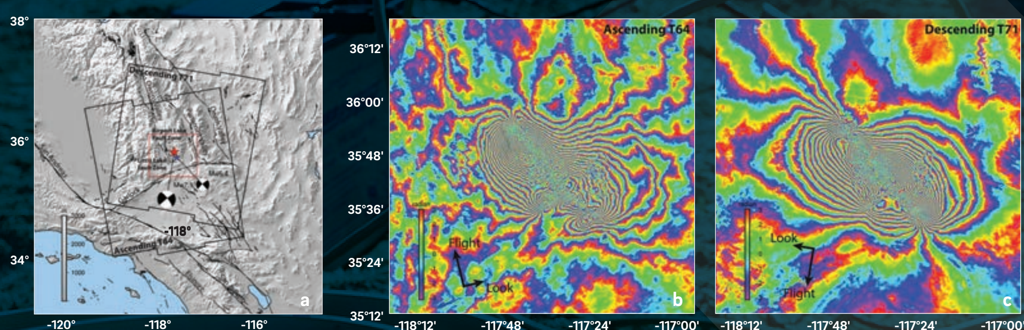

(a) Overview map of the topography, faults, and Sentinel-1 frames surrounding the 2019 Ridgecrest earthquake sequence. Red and blue stars denote the epicenter of the Mw 7.1 and Mw 6.4 earthquakes, respectively. Black curves are faults mapped by United States Geological Survey. (b) Interferogram from the descending track 71 Sentinel-1 InSAR data. (c) Interferogram from the ascending track 64 Sentinel-1 InSAR data.

PLUM EARTHQUAKE EARLY WARNING ALGORITHM

Dr. Kilb is part of a research team studying the Propagation of Local Undamped Motion (PLUM) earthquake early warning algorithm, originally designed for use in Japan, that has also been shown effective at detecting quakes in Southern California (Cochran et al., 2019). The PLUM algorithm is now being consider for inclusion of the USA West Coast (California, Oregon, and Washington) ShakeAlert earthquake early warning system, a system designed to detect significant earthquakes quickly and issue alerts to people before shaking arrives at their location. ShakeAlert does not predict earthquakes. The goal of ShakeAlert is to detect large earthquakes, calculate ground motion intensities and provide timely alerts to people and infrastructure deemed to potentially be in harm's way (see https://www.shakealert.org).

Differing from current ShakeAlert algorithms, PLUM is ground-motion-based and designed to issue alerts when the observed ground motions exceed a specified intensity. Currently, PLUM is station-based, requiring two neighboring stations to report large ground motions. PLUM only reports the location of large ground motions, it does not report earthquake magnitude or location as in the current ShakeAlert algorithms. In this way, PLUM can detect relatively small magnitude quakes (Magnitude<4) that produce ground motions above the ShakeAlert alerting threshold (Modified Mercalli Intensity >=4).

The July 2019 M6.4 and M7.1 Ridgecrest earthquakes provided an opportunity for PLUM to be tested in real-time, assessing the alert's timeliness and accuracy (lead author Dr. Sarah Minson). We found that PLUM successfully sent alerts for both earthquakes with latencies (including telemetry) of 5 and 7 seconds, respectively, on par or better than the production ShakeAlert algorithms EPIC and FinDer. These real-time tests included data latencies of the operational ShakeAlert earthquake early warning system, which was especially important because the high data latencies during the M7.1 earthquake degraded ShakeAlert's performance. PLUM proved to be largely immune to these latency issues.

Using three different alerting strategies, we found that PLUM was able to accurately forecast shaking across southern California. As would be expected, a benefit-cost analysis of each approach illustrates trade-offs between increasing warning time and minimizing the area receiving unneeded alerts. Choosing an optimal alerting strategy requires knowledge of users' false alarm tolerance and minimum required warning time for taking protective action.

Read Further: Cochran, E. S., J. Bunn, S.E. Minson, A.S. Baltay, D. Kilb, Y. Kodera and M. Hoshiba [2019]. Event detection performance of the PLUM earthquake early warning algorithm in Southern California. *Bull. Seism. Soc. Am.,* doi: 10.1785/0120180326.

SCIENCE AT SEA: IGPP CRUISES

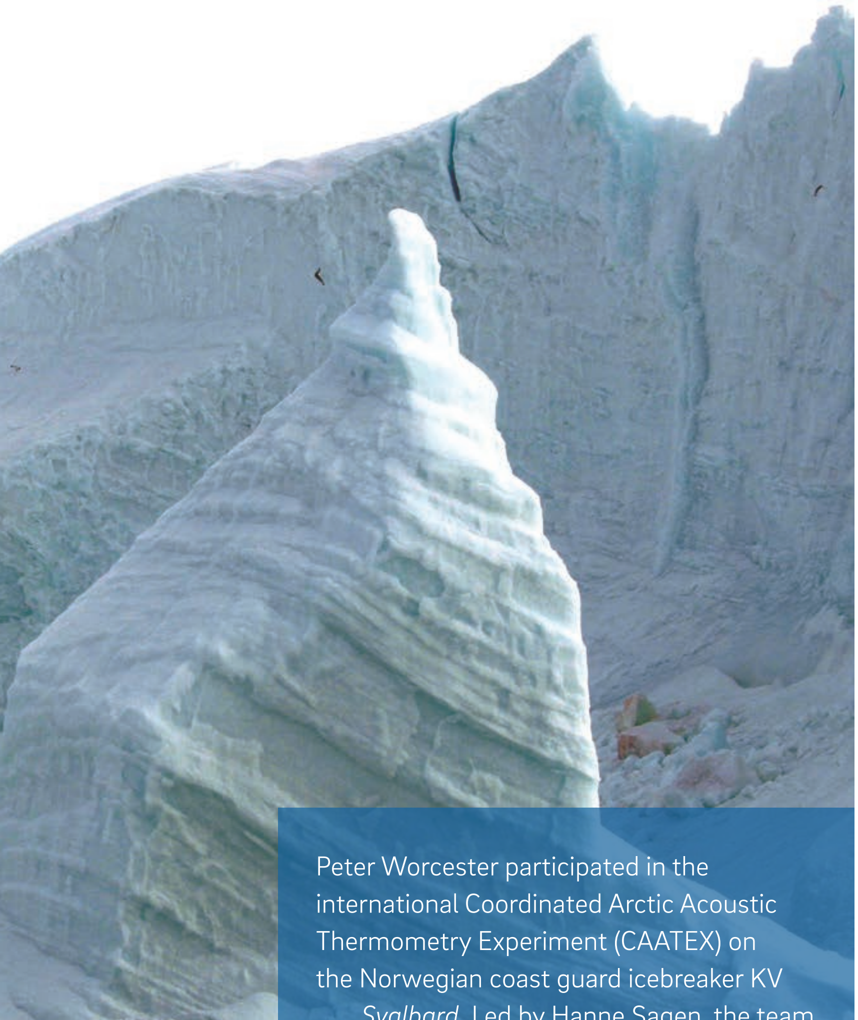

Peter Worcester participated in the international Coordinated Arctic Acoustic Thermometry Experiment (CAATEX) on the Norwegian coast guard icebreaker KV *Svalbard.* Led by Hanne Sagen, the team reached the North Pole on August 19 and deployed low-frequency sound source moorings into the Eastern Arctic.

For CAATEX program details, visit: https://caatex.nersc.no.

Matt Dzieciuch joined a Coast Guard team on the USCGC *Healy* in the Western Arctic to deploy 3 low-frequency (35 Hz) sound source moorings. Partners, aboard the K/V *Svalbard,* led by Hanne Sagen (and including Peter Worcester) at the Nansen Environmental and Remote Sensing Center deployed similar moorings in the Eastern Arctic. The goal was to repeat a similar experiment conducted 25 years ago to determine the continued spread of warm and salty Atlantic water through the middle of the Arctic ocean water column.

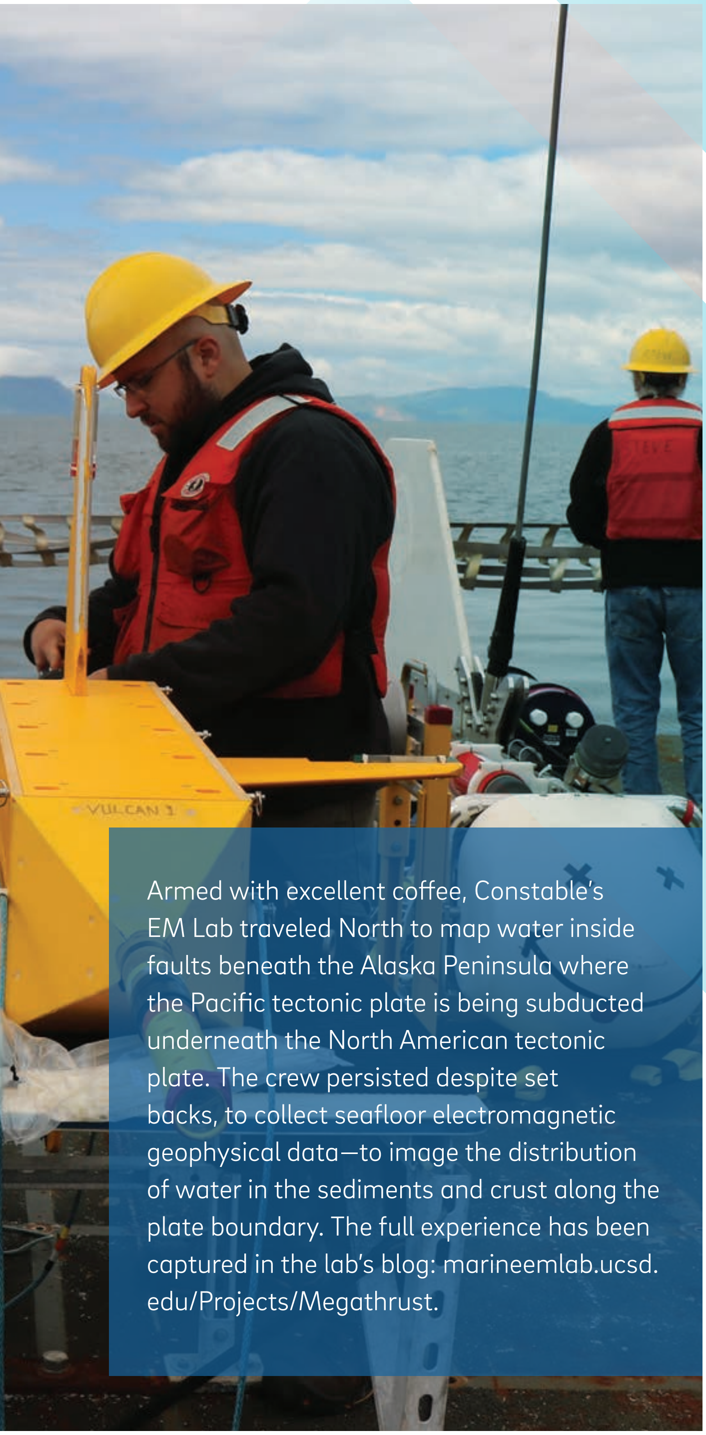

Armed with excellent coffee, Constable's EM Lab traveled North to map water inside faults beneath the Alaska Peninsula where the Pacific tectonic plate is being subducted underneath the North American tectonic plate. The crew persisted despite set backs, to collect seafloor electromagnetic geophysical data—to image the distribution of water in the sediments and crust along the plate boundary. The full experience has been captured in the lab's blog: marineemlab.ucsd.edu/Projects/Megathrust.

AUTONOMOUS SYSTEMS IN OCEANOGRAPHY

John Orcutt, Jonathan Berger, Jeff Babcock, Gabi Laske

Affordable systems for agile, ocean-based research

The sophistication of measurements in oceanography is growing at a rapid rate with the construction of new instruments characterized by advanced electronics, artificial intelligence, higher-capacity batteries and new approaches involving advanced composite materials. At the same time, the construction of new ships and platforms challenge both construction and operational costs. The use of large oceanographic ships, largely constructed by the US Navy, has introduced new challenges to oceanographers. Research budgets are increasing at rates on the order of 2%/year—often less that the general economy. The allocation of funds at the NSF Ocean Sciences for infrastructure has decreased to meet a target of 50/50 for infrastructure relative to scientists' salaries. This can be compared for 80/20 for Astronomy and 20/80 for Earth sciences. New approaches to instrument engineering are essential to maintain a vibrant knowledge return in oceanography.

The Navy faces a similar problem in terms of new ships. Personnel costs are growing rapidly in terms of increasing salaries and shrinking availability of qualified personnel. The Navy has built a small number of autonomous ships and has substituted technology for sailors. The Sea Hunter is an entirely autonomous ship that costs $15,000 - $20,000/day at sea while a destroyer costs $700,000/day to operate. The daily cost for a large oceanographic ship such as the R/V *Roger Revelle* is now $50,000/day and the R/V *Marcus Langseth* costs much more than this.

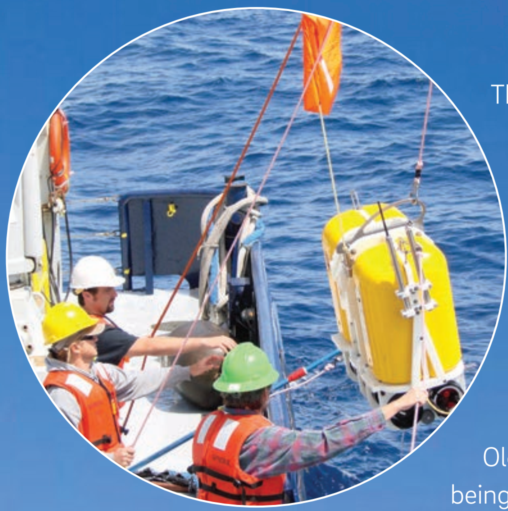

The future of oceanography depends upon making systems more autonomous. We are constructing a new version of a Seafloor Gateway based on a Boeing Sea Glider. Seismometers and geodetic systems on the seafloor telemeter their data to the surface glider via acoustics. The data are then passed along to shore using satellite telemetry. The new gateways will exploit Low Earth Orbit (LEO) and Mid Earth Orbit (MEO) satellites to allow growth in data rates and reduce latency.

Older approaches in constructing seafloor instruments are being replaced with new composite systems. Older instruments were often built with glass ball floatation, blocks of syntactic foam, and aluminum struts to hold everything together. The new instruments are constructed using composites and syntactic foam that are spun from raw composites to minimize costs while eliminating bolts, metals and screws that corrode rapidly and introduce noise that challenges quiet measurements at seismic and geodetic frequencies on the seafloor. Instrument lifetimes are greatly increased and are now in common use including the fifteen Trawl-Resistant ABALONES. These new instruments are now available commercially from Nanometrics near Ottawa in Canada.

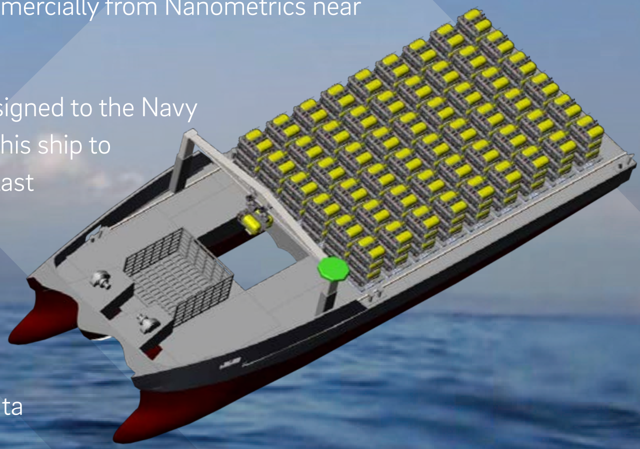

The original Navy autonomous ship (Sea Hunter) is now assigned to the Navy in San Diego. We are working with the company that built this ship to realize an autonomous oceanographic ship depicted in the last figure. There are 324 seafloor seismometers on deck, one of which is being launched from the gantry crane that travels fore and aft. Recovery of all the instruments would be accomplished in reverse order. The green hexagonal synthetic aperture antenna is used for high bandwidth MEO/LEO communications with shore for passing along data and solving problems.

Seismic power spectra in the last figure depict quiet seafloor noise measured with a broadband Ocean Bottom Seismograph in the Pacific, west of Hawaii. The blue seismic spectra depict vertical acceleration spectra while the red spectra represent quiet island measurements from Kipapa in Hawaii. The noise levels on the seafloor are low and achievable with modern seafloor systems used regularly in our research. Autonomous systems can be used to expand significantly continuous measurements that are presently made in the 25% of the planet covered by continents. Significant enhancements of 3D structure of Earth are now realistic with modern technology.

STUDYING THE SKY // ATMOSPHERIC WAVE DYNAMICS

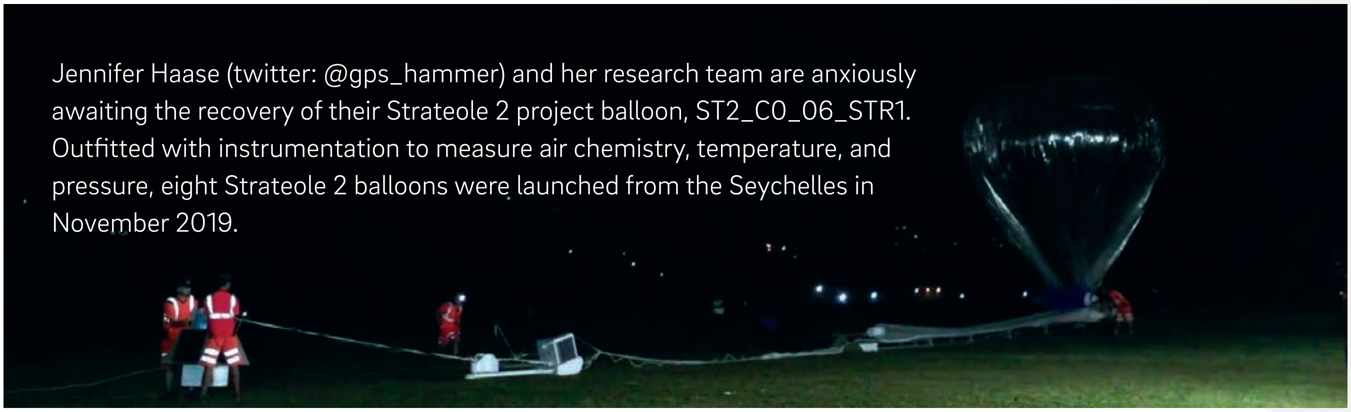

Jennifer Haase (twitter: @gps_hammer) and her research team are anxiously awaiting the recovery of their Strateole 2 project balloon, ST2_CO_06_STR1. Outfitted with instrumentation to measure air chemistry, temperature, and pressure, eight Strateole 2 balloons were launched from the Seychelles in November 2019.

ST2_CO_06_STR1 finished it's journey (slightly off course) on Mali where a search for the payload is planned shortly.

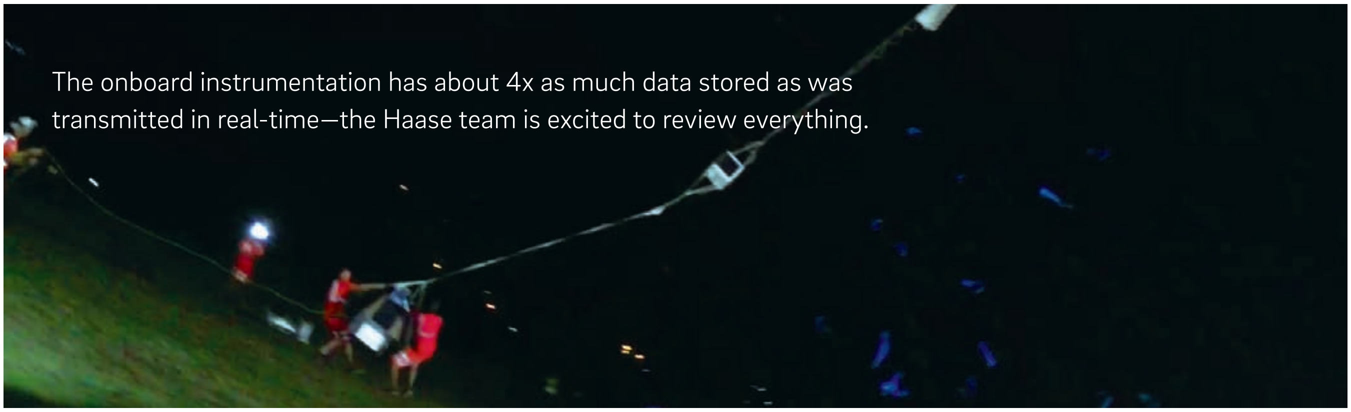

The onboard instrumentation has about 4x as much data stored as was transmitted in real-time—the Haase team is excited to review everything.

Supported by the National Science Foundation, the French National Center for Scientific Research and the French Space Agency, the balloons have been equipped to gather data that will further the understanding of atmospheric waves dynamics and help scientists further refine climate models to better predict climate trends.

Learn more about the Strateole 2 project and track the Haase team's balloon, ST2_CO_06_STR1 (in yellow): https://webstr2.lmd.polytechnique.fr/#/.

GEOPHYSICS CURIOUS?

Students in the IGPP graduate program study Earth and other planets to advance our fundamental understanding their origin, composition, and evolution, and explore the implications for life, for the environment, and for society. The graduate program provides a broad education in the fundamentals of geophysics, alongside research and coursework spanning multiple specializations.

Our multidisciplinary program offers graduate students a unique hands-on, collaborative learning environment. In addition to our core academic curriculum, we emphasize linking observational techniques and the collection of novel datasets for testing new theoretical and computational approaches. GP students participate extensively in field experiments, instrument development, laboratory investigations, and shipboard expeditions. Graduates go on to careers in research, education, industry, and public policy. Scripps has strong working relationships with the NSF, NASA, NOAA, the USGS, and the Office of Naval Research, and can provide graduates with long-term networking and professional support.

Is this graduate program for you? Read about some ongoing research in the following pages and learn more about the program online: igpp.ucsd.edu/program-study.

DUNCAN CARR AGNEW

Professor

dagnew@ucsd.edu, 858-534-2590

Crustal deformation measurement and interpretation, Earth tides, Southern California seismicity, history of science.

As noted in last year's report, all funding for the operation of the long-base laser strainmeters ended on October 31, 2018. Considerable work has been done towards papers reporting the results from these instruments, but this and other work were impacted by major University service. Over the last three years I have helped two other groups, in Hillers et. al (2019), understanding the strainmeter data, and in Inbal et. al (2018), pointing out the existence and behavior of a 3-Hz noise peak seen on borehole seismometers in the Anza area, which appears to be produced by truck traffic. I have also written two historical papers: Agnew (2018) on how the New Madrid earthquake was and was not remembered, and Agnew (2020) on the history of seismological timekeeping.

RECENT PUBLICATIONS

Agnew, D. C. (2018). Forgetting and remembering the New Madrid earthquakes, *Earth Sciences History*, ***37***, 177-202, 211-212.

Inbal, A., T. Cristea-Platon, J.-P. Ampuero, G. Hillers, D. Agnew, and S. E. Hough (2018). Sources of long-range anthropogenic noise in Southern California and implications for tectonic tremor detection, *Bull. Seismol. Soc. Am.*, ***108***, 3511-3527, 10.1785/0120180130

Hillers, G., M. Campillo, F. Brenguier, L. Moreau, D. C. Agnew, and Y. Ben-Zion (2019). 'Seismic velocity change patterns along the San Jacinto fault zone following the 2010 M7.2 El Mayor-Cucapah and M5.4 Collins Valley earthquakes, *J. Geophys. Res. Solid Earth*, ***124***, 7171-7192, 10.1029/2018JB017143

Agnew, D. C. (2020) Time marks and clock corrections: A century of seismological timekeeping, *Seismol. Res. Lett.* ***91***, 10.1785/0220190284

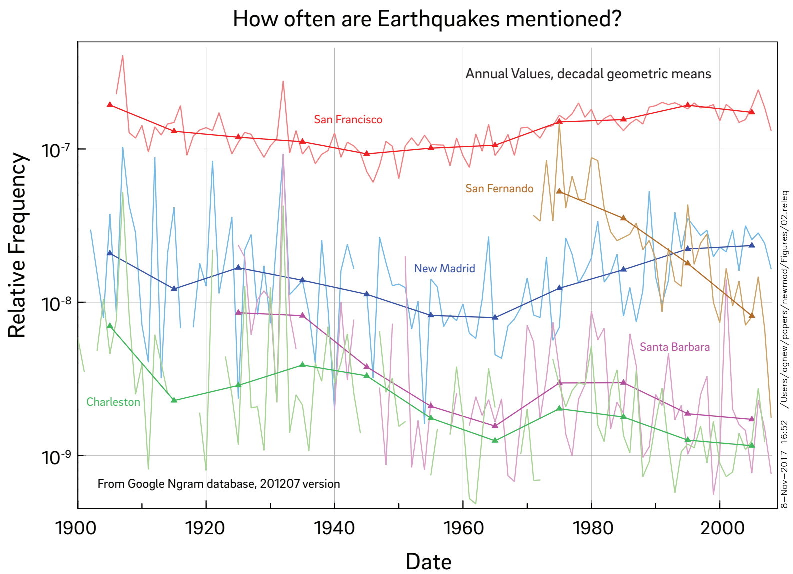

Figure 1. Frequency of occurrence of specific earthquake names in the Google Ngrams database of English language books (version 2, July 2012. Light lines show year-by-year variations, heavy lines with symbols decadal averages.

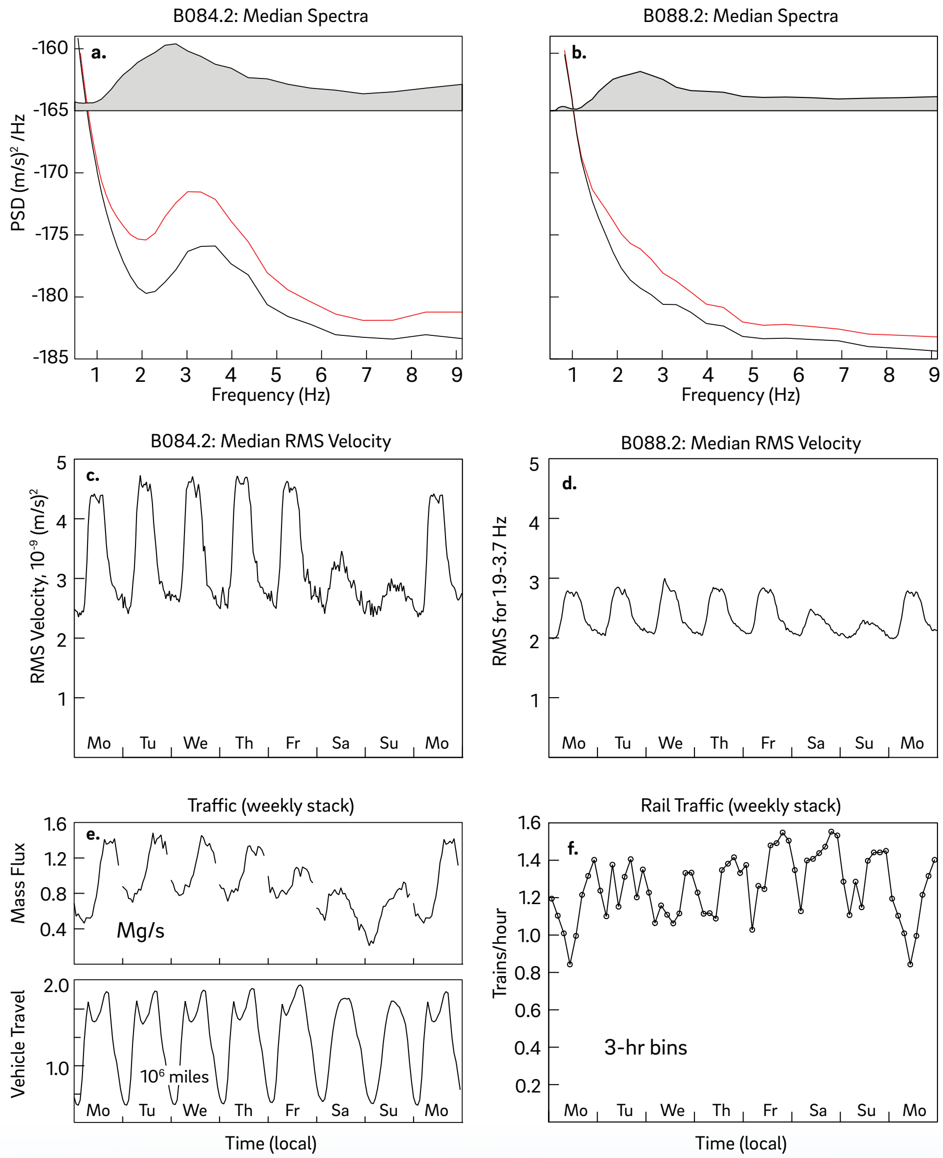

Figure 2. Properties of the 3 Hz hum observed on stations of the PBO network in the Anza area. Panels (a) and (b) show median power spectra of a horizontal component at two PBO sites. In each panel, the red line shows the median spectrum for times from 0900 to 1500 (local time) on weekdays; the black line shows the median spectrum for times from 2100 to 0300 on all nights. The filled area shows the difference between these. Panels (c) and (d) show the time variation of the spectrum integrated over frequencies from 1.7 to 3.9 Hz, where the largest peak is X. The values are medians for rms values binned at 36 minute and folded to be days of the week; each median uses about 700 individual values. Panel (e) shows two measures of highway traffic total vehicle miles traveled on State highways in Caltrans District 8 (Riverside and San Bernardino counties), truck traffic through a weighing station; both are hourly averages, for the total over the timespan 2010:060-099 and for trucks 2010:077-110. Panel (f) shows average rail traffic on the Yuma Division of the Union Pacific Railroad based on detections at the Durmid Hill laser strainmeter for 2008 through 2011.

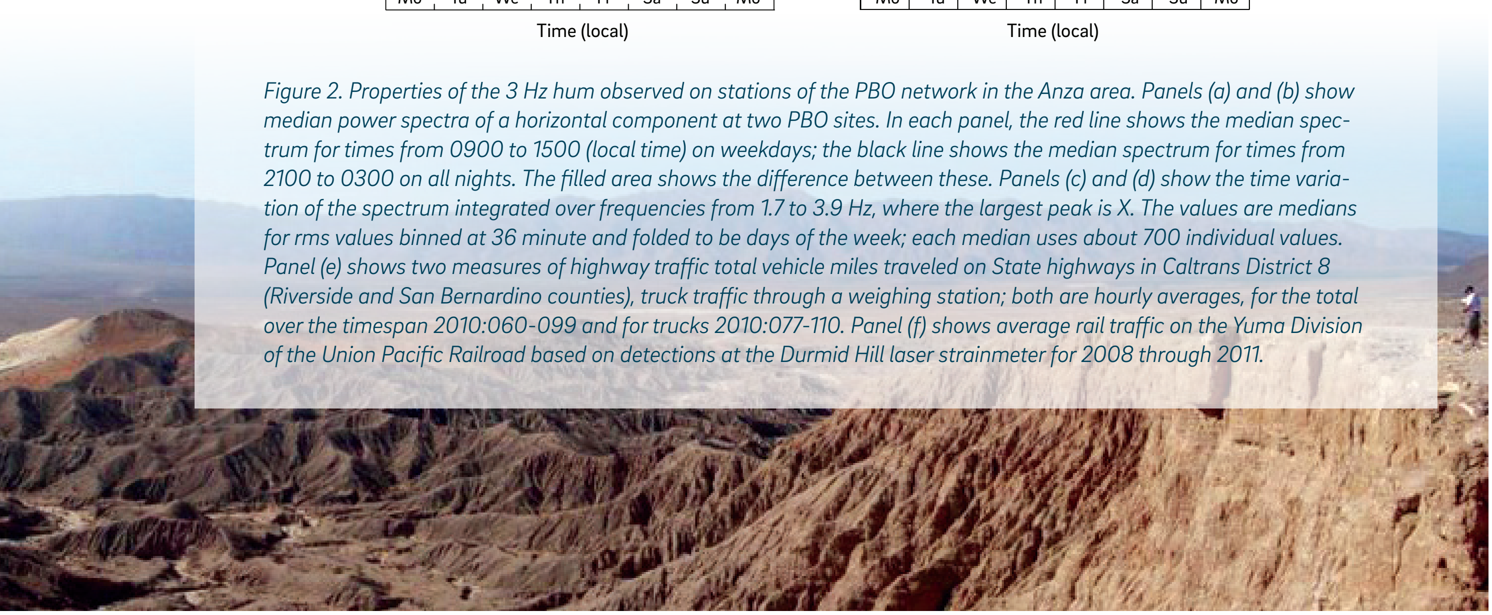

JONATHAN BERGER

Emeritus Researcher, RTAD

jberger@ucsd.edu, 858-534-2889

Global seismological observations, marine seismo-acoustics, geophysical instrumentation, deep ocean observing platforms, ocean robotics, global communications systems

This year my colleagues and I, in collaboration with the US Geological Survey implemented a substantial upgrade of the underground facilities at Pinyon Flat Observatory (PFO). Specifically, three 100-m deep GSN-style boreholes, fully cased and cemented, were drilled by a team USGS drilling team from Las Vegas. In the locations shown in Figure 1.

Figure 3. Map of PFO showing the locations of proposed new holes (SDF, SDG, and SDH) with yellow pins, trenches connecting these holes to existing power/communications infrastructure as white lines, and the location of two pre-existing holes (SDC, SDT) were modified.

One of these boreholes is being prepared for installation of the Optical seismo-geodetic instrument while the others are intended for installation of the new broadband seismometers developed by Kinemetrics and Nanometrics. The first such installation features two such seismometers installed in the same borehole, The figure below shows spectra of some recent results for the east components of various seismometers: the PFO STS1 and PFO T240 are both installed on the pier in the underground facility in the northeast vault, the XPFO T360 is installed in a post hole drilled in the floor of that underground vault at a depth of 15m beneath the ground surface. The XPFO STS5A and STS-6 are those installed in the same borehole at a depth of 9.8 m and 76.40m respectively.

Figure 4. Drill team on site.

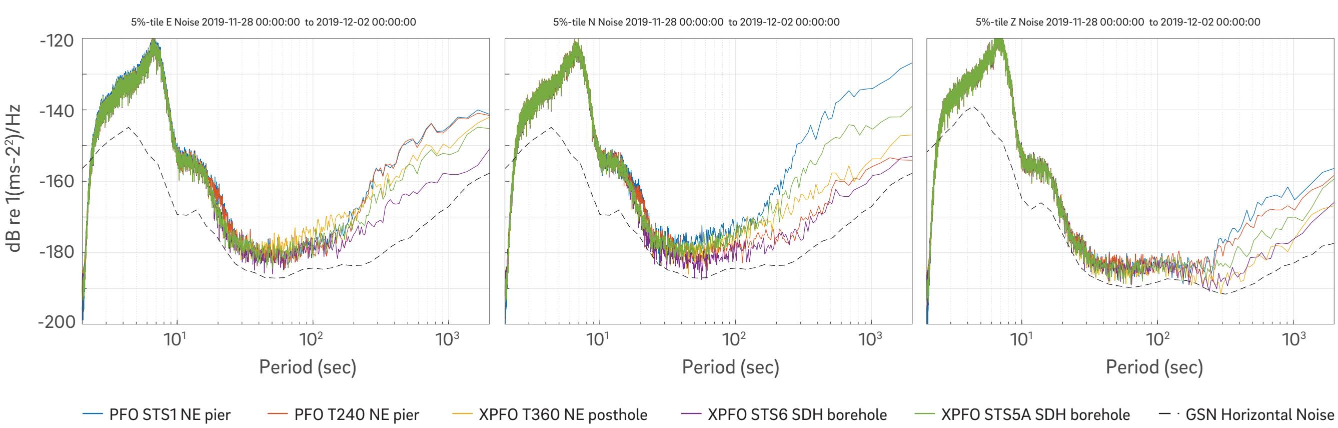

YEHUDA BOCK

Distinguished Researcher and Senior Lecturer; Director, Scripps Orbit and Permanent Array Center (SOPAC); Director, California Spatial Reference Center (CSRC)

ybock@ucsd.edu, 858-534-5292

GPS/GNSS, crustal deformation and transients, geodetic reference frames, early warning systems for earthquakes and tsunamis, seismogeodesy, GPS meteorology, structural health monitoring, data science, MEMS sensors

The SOPAC group's current focus includes the combined use of seismic and geodetic methods to support natural hazard mitigation for communities affected by earthquakes, tsunamis, volcanoes, and severe weather. The research is aided by in-house instrument design, field deployment of sensor packages, real-time data collection and analysis, development of rapid hazard characterization methods, and interaction with hazard warning centers. Using 25+ years of geodetic displacement time series, we also study tectonic signals of interest (see Figures), including interseismic, coseismic and postseismic deformation, and transients such as fault creep, subsidence and episodic tremor and slip (ETS). SOPAC also archives GNSS metadata and data products with accompanying IT infrastructure and database management system for the International GNSS Service and the California Spatial Reference Center. Over the last year, the SOPAC group included Peng Fang, Songnian Jiang, Allen Nance, Anne Sullivan, Maria Turingan, Wang Hu, Dorian Golriz, and postdoctoral researchers Dara Goldberg and Emilie Klein, with laboratory and field assistance by Matt Norenberg and Glen Offield.

TRANSIENT DEFORMATION AND REFERENCE FRAMES

It is challenging to maintain a geodetic reference in the presence of crustal motion including steady secular motions and transient motions at various spatial and temporal scales (Figure 5). Our focus at SOPAC is California, which sits on the boundary of the North America and Pacific plates resulting in a steady ("secular"), primarily horizontal motion on the order of up to 50 mm/yr on the San Andreas Fault System distributed over a width of hundreds of kilometers. North of Cape Mendocino, the tectonic regime changes from primarily strike slip motion to thrust faulting along the Cascadia Subduction Zone. This steady motion is punctuated by significant earthquakes that may instantaneously cause up to a meter of motion near the earthquake's epicenter followed by significant postseismic motion over a period of months to years until the crust returns to its steady state. Since 1992, California addition to the 2019 Ridgecrest events, California has experienced twenty earthquakes from magnitudes 5.1-7.2 that significantly affected the positions of one to hundreds of stations. For example, the April 4, 2010 Mw 7.2 El Mayor-Cucapah in northern Baja California, Mexico caused significant coseismic motion (up to 0.3 meters) throughout southern California and an additional cumulative postseismic motion of about 50% nearly over a decade. Other transient motions are related to tectonic and magmatic processes and vertical land motion (subsidence and uplift) due to natural (e.g., drought) or anthropogenic (e.g., water and oil extraction) effects (Figure 6) (Klein et al., 2019).

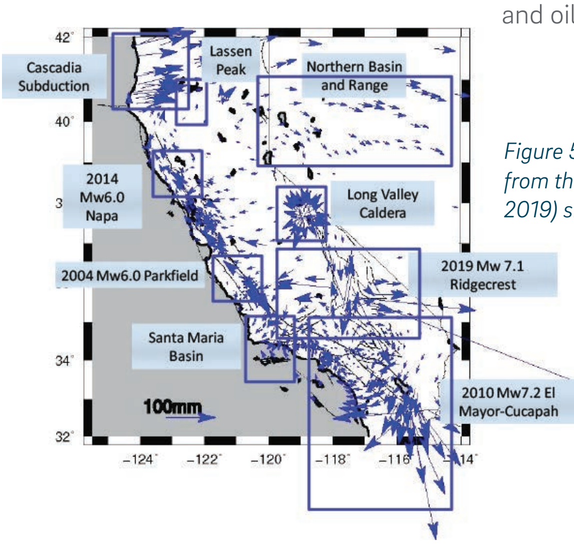

Figure 5. Transient Horizontal Motions. Accumulated residual horizontal displacements from the start of 2010 until mid-October, 2019 for California and Nevada (Klein et al., 2019) showing transients and secular differences with the secular model of Zeng and Shen (2017). The weekly accumulation of the gridded displacement residuals forms the basis for defining a kinematic reference frame for California (Bock and Klein. 2018). We see significant secular differences with the model, for example, in Cascadia, the Northern Basin and Range, and the Santa Maria basin, that can then be used for further secular fault slip models. Transients include postseismic motion for 4 earthquakes in this 10-year period, and the horizontal expression of magmatic inflation at Long Valley Caldera and Lassen Peak (Bock et al., 2019).

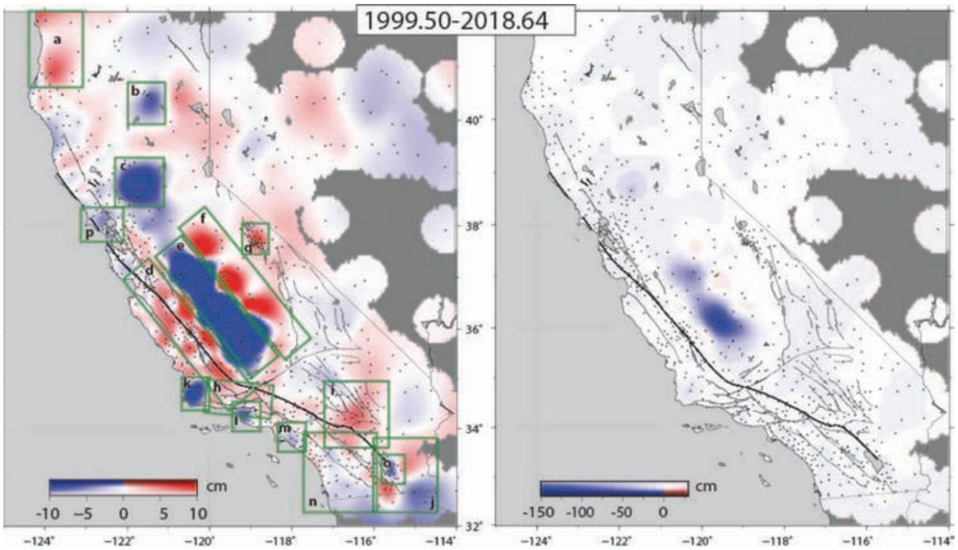

Figure 6. ***Transient Vertical Motions.*** *Accumulated vertical displacement field between 1999.5 and 2018.6, represented with two different color scales to highlight significantly greater vertical motion in the Central Valley (Zone e). Zones a-n with significant vertical motion are defined in Klein et al. (2019).*

RECENT PUBLICATIONS

Bock, Y. and E. Klein (2018), Investigations into a Dynamic Datum for California, Final report to California Department of Transportation (Caltrans), June 22.

Goldberg, D. E., D. Melgar, Y. Bock, R. M. Allen (2018), Geodetic Observations of Weak Determinism in Rupture Evolution of Large Earthquakes, *J. Geophys. Res.,* 123, https://doi.org/10.1029/2018JB015962.

Klein, K., Y. Bock, X. Xu, D. Sandwell, D. Golriz, P. Fang, L. Su (2019), Transient deformation in California from two decades of GPS displacements: Implications for a three-dimensional kinematic reference frame, *J. Geophys. Res.,* DOI:10.1029/2018JB017201.

Rowan, L. (2019), Capturing California's Crustal Motion with Geodesy, UNAVCO Science Snapshots, https://www.unavco.org/science/snapshots/solid-earth/2019/klein.html

Murray, J. R. et al. (2019) Regional Global Navigation Satellite System Networks for Crustal Deformation Monitoring, *Seismo. Res. Lett.* https://doi.org/10.1785/0220190113

Wang M., J. Wang, Y. Bock, H. Liang, D. Dong, P. Fang (2019), Dynamic Mapping of the Movement of Landfalling Atmospheric Rivers over Southern California with GPS Data, *Geophys. Res. Lett,* 46. https://doi.org/10.1029/2018GL081318.

ADRIAN BORSA

Assistant Professor

aborsa@ucsd.edu; 858-534-6845

Remote hydrology from joint analysis of GPS/GNSS, GRACE and InSAR. Transient surface deformation from natural and anthropogenic sources using InSAR and GNSS. Noise sources in geodetic remote sensing, calibration/validation of geodetic observations, and optimal combinations of geodetic information. Differential lidar techniques applied to problems in geomorphology and tectonic geodesy. Dry lake geomorphology. Socioeconomic responses to water scarcity and implications for public policy.

Much of my current research involves the characterization of the hydrological cycle using observations of Earth surface deformation and mass distribution. Specifically, I am interested in observing and analyzing changes in terrestrial water storage (the total water in glaciers, snowpack, lakes, soil, and groundwater) which are critical to closing the water budget but which have been poorly observed until recently. My group combines satellite gravity measurements of water mass change (from the GRACE mission) with GNSS observations of crustal deformation associated with these water mass changes to recover the evolution of water storage across the continental USA and beyond. While seasonal signals from hydrology have been extensively studied, changes over both shorter and longer periods have not been broadly documented. We use a variety of techniques to investigate spatiotemporal patterns of water storage in watersheds across the United States, the extent and duration of droughts, and watershed flooding/recovery from storms such as Hurricane Harvey.

We are also investigating linkages between water and the solid earth, including possible triggering of seismicity (the L'Aquila, South Napa and El Mayor–Cucapah earthquakes) and volcanism (Long Valley Caldera) by water-related crustal stresses. These studies often incorporate InSAR (interferometric synthetic aperture radar) observations of subsidence from groundwater extraction, which provide high spatial resolution and broad coverage of impacted areas. Additionally, we are using our InSAR time series over California's Central Valley in a collaboration with colleagues at UC San Diego's School of Global Policy and Strategy to study crop selection and planting decisions in response to changes in rainfall, surface water deliveries, and groundwater availability.

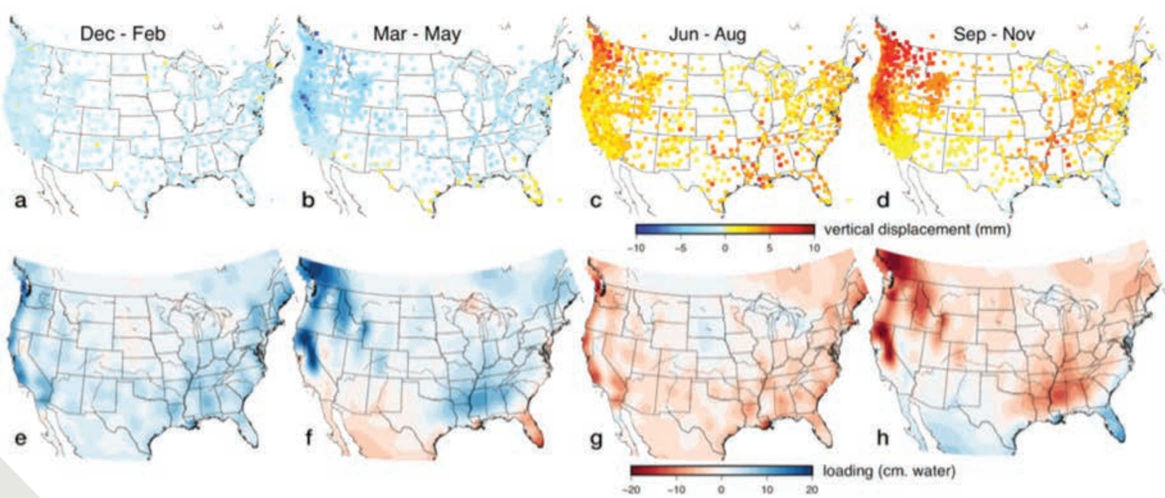

Figure 7. (a-d) Seasonal vertical displacements from GPS across the continental United States (CONUS), showing overall subsidence (cool colors) in the winter and spring, and uplift (warm colors) in the summer and fall. (e-h) Estimated terrestrial water storage anomalies (TWSA) corresponding to panels a-d, from joint analysis of GPS and GRACE data. TWSA typically peaks in winter-spring and is smallest in summer-fall, except on the southern/southeastern CONUS boundary (e.g. Florida and the Gulf and Atlantic coasts), where the seasonal phase is advanced by 3 months.

Another primary area of research has been the calibration and validation (cal/val) of satellite altimeter measurements. In collaboration with SIO colleague Helen Fricker, my group used kinematic GNSS to survey Bolivia's salar de Uyuni in 2002, 2009 and 2012 to create a digital elevation model (DEM) of the surface. Using this reference DEM, we identified a significant error in ICESat processing whose correction changes ICESat-derived elevation change trends for the stable portions of the Greenland and Antarctic ice sheets. We later found a previously unidentified 5 cm bias between ICESat's lasers, whose magnitude is larger than the elevation error budget for the mission.

We are now linking absolute GPS measurements with relative motions provided by InSAR to provide a time series of surface displacements for cal/val and for studying salar geomorphology. We have also expanded our cal/val activity to the CryoSat mission, are currently collaborating with European investigators doing cal/val for SWOT, and are about to begin cal/val analysis for ICESat-2.

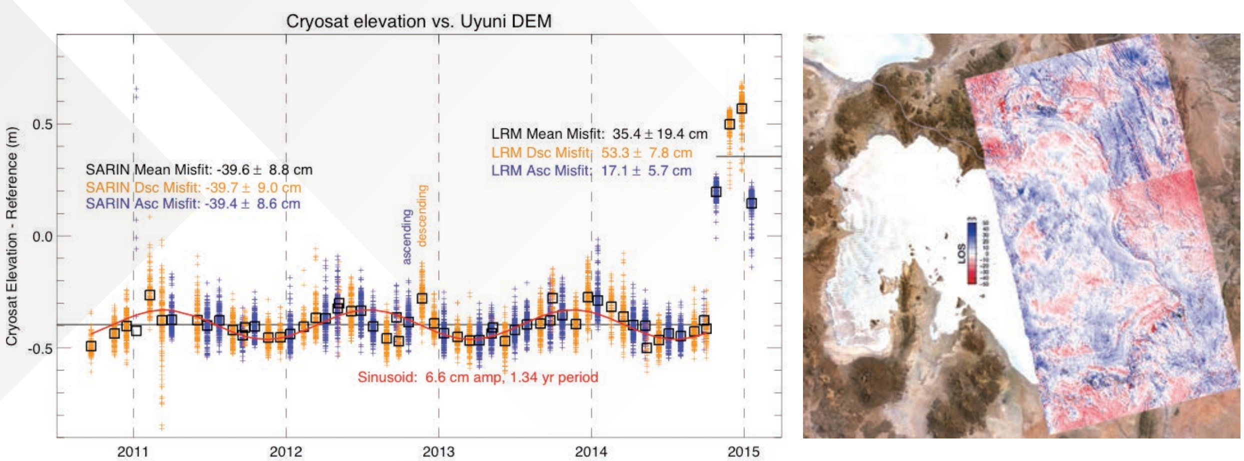

Figure 8. Left: Cryosat elevation validation relative to the salar de Uyuni DEM, with residuals showing a.) a uniform range bias of -40 cm for SARIN mode and +35 cm for LRM mode, b.) an 7 cm amplitude sinusoidal anomaly of 1.34 yr period that is still unexplained, and c.) higher range resolution than reported elsewhere, even with the sinusoidal anomaly. Right: ALOS InSAR results over the salar de Uyuni for the period 8/27/2010 - 1/12/2011, indicating that seasonal elevation change is <1 cm averaged over the salar surface.

RECENT PUBLICATIONS

Adusumilli, S., A.A. Borsa, M.A. Fish, H.K. McMillan, and F. Silverii (2019). "A Decade of Water Storage Changes Across the Contiguous United States from GPS and satellite gravity." *Geophysical Research Letters,* ***46***(22)

Borsa, A., H.A. Fricker, K. Brunt (2019). "A terrestrial validation of ICESat elevation measurements." *IEEE Transactions on Geoscience and Remote Sensing,* ***57***(9)

Enzminger, T.L., E. E. Small, A.A. Borsa. "Subsurface water dominates Sierra Nevada seasonal hydrologic storage." *Geophysical Research Letters,* ***46***(21)

Kramer, M., W. Holt, A. Borsa, (2018). "Seasonal non-tectonic loading inferred from cGPS as a potential trigger for the M6. 0 South Napa Earthquake." *Journal of Geophysical Research: Solid Earth,* ***123***(6), 5300-5322

Neely, W.R., A.A. Borsa, F. Silverii (2019). "GInSAR: A cGPS correction for enhanced InSAR time series." *IEEE Transactions on Geoscience and Remote Sensing,* ***58***(1)

Silverii, F., D'Agostino, N., Borsa, A.A., Calcaterra, S., Gambino, P., Giuliani, R. and Mattone, M. (2019). "Transient crustal deformation from karst aquifers hydrology in the Apennines (Italy)." *Earth and Planetary Science Letters,* ***506***, 23-37

Trugman, D.T., Borsa, A.A. and Sandwell, D.T. (2014) "Did stresses from the Cerro Prieto Geothermal Field influence the El Mayor-Cucapah rupture sequence? *Geophysical Research Letters,* ***41***(24), 8767-8774

CATHERINE CONSTABLE

Distinguished Professor of Geophysics

cconstable@ucsd.edu, 858-534-3183

Earth's magnetic field and electromagnetic environment; Paleo and geomagnetic secular variation; Linking paleomagnetic observations to geodynamo simulations; Paleomagnetic databases; Electrical conductivity of Earth's mantle; Inverse problems; Statistical techniques.

The natural spectrum of geomagnetic variations at Earth's surface extends across an enormous frequency range and is dominated by low frequency changes, associated with the predominantly dipolar internal field produced by the geodynamo in Earth's liquid outer core. Fluid flow and diffusive processes in the electrically conductive core produce secular variation in the magnetic field. The dipole part of the field exhibits the largest changes, associated with geomagnetic excursions and reversals which require the axial dipole part of the field to vanish as it changes sign. Finite electrical conductivity of the mantle effectively filters variations in the core field on time scales much less than a year. Satellite observations and ground based observatory data can be used to study geomagnetic variations on the timescales of the solar cycle, and are used for studies of deep mantle electrical conductivity. Paleomagnetic data from volcanics, archeomagnetic artifacts, and sediments provide information on longer time periods ranging from hundreds to millions of years.

My recent research has mainly been focused on understanding the evolution of the geomagnetic field over 0–100 ka, a time interval which is long enough to represent paleosecular variation and several geomagnetic excursions, during which the geomagnetic dipole strength drops and global or regional field direction show large departures from their more usual stable polarity configurations.

The Laschamp excursion appears to be the only event with a strong global signature during the past 100 kyr. In work together with Sanja Panovska and Monika Korte (of GeoForschungs Zentrum, Helmholtz Center, Potsdam), we have conducted a study of field structure during the Laschamps excursion which occurred around 40 ka and of other regional excursional events. As shown in Figure 9 this raises a renewed possibility of spatial concentrations of VGP aths during geomagnetic excursions which we are continuing to investigate.

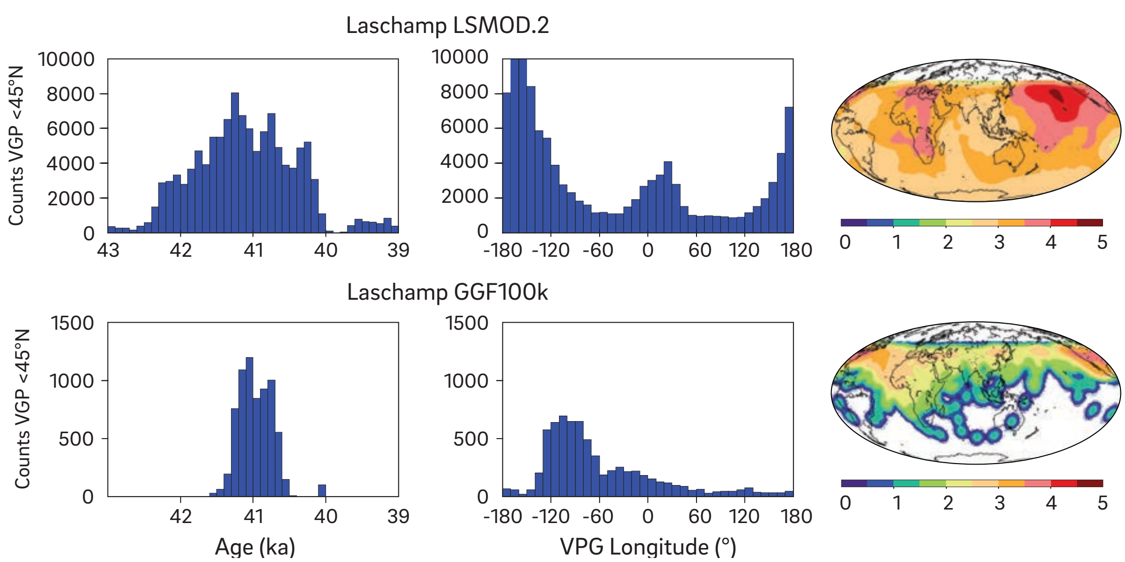

Figure 9. Left: Age and longitude distributions for transitional (< 45 latitude) virtual geomagnetic pole (VGP) positions during the Laschamp excursion from 43-39 ka in the GGF100k and LSMOD.2 models of time variations in the geomagnetic field. Right: Spatial concentrations of VGPs may reflect the influence of geographic variations in core-mantle boundary conditions on the geodynamo.

Work with Christopher Davies (Leeds University, U.K.) is continuing on linking numerical geodynamo simulations with paleomagnetic results, especially in the analysis of rapid changes in the magnetic field. Broad similarities between behavior in the paleofield and numerical simulations allow us to link potential physical processes in the simulations with actual field behavior that is not easily resolvable from paleomagnetic data and models.

In an additional topic of interest I have been revisiting statistical models of geomagnetic paleosecular variation (PSV) in collaboration with Daniele Brandt of Sao Paolo University, Brazil. As a result of much earlier work at Scripps we developed the Giant Gaussian Process model, a successful prototype for describing statistical distributions of temporal variations in the field over the past 5 million years. The GGP model has been through several iterations as newly compiled data sets have revealed limitations in its simplest versions. Current version still rely on a time averaged field represented by a geocentric axial dipole, and simple partitioning of PSV into parts that are symmetric and antisymmetric about the equator. Improvements in diagnostic tests show that paleomagnetic data from Antarctica present a significant challenge to these simple models for the 0-5 Ma interval, and further developments will be needed. In other work we have been assessing whether paleomagnetic data from the Kiaman Reverse Polarity interval (extending from 262 to 318 Ma) may be compatible with GGP type models. It may be possible

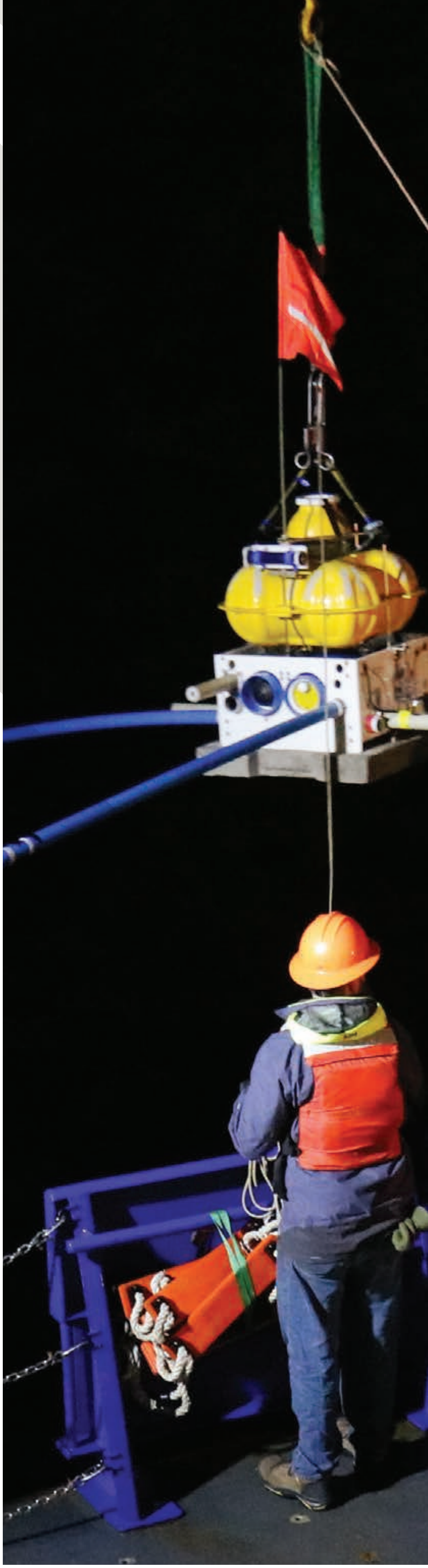

RECENT PUBLICATIONS

Avery, M.S., C.G. Constable, C.J. Davies, D. Gubbins, 2019. Spectral methods for assessing energy balances in numerical geodynamos, *Phys. Earth Planet. Inter.*, ***286,*** 127–137 , doi:10.1016/j.pepi.2018.10.002

Brandt, D., Marcia Ernesto, Catherine Constable, Daniel Ribeiro Franco, Luiz Carlos Weinschutz, Pillar de Oliveira Carvalho Rodrigues, Linda Hinnov, Plinio Jaqueto, Beck Strauss, Joshua Feinberg, Pedro Vitor de Paiva Franco, Xixi Zhao, 2019. New late Pennsylvanian paleomagnetic results from Parana Basin (southern Brazil): Is the recent Giant Gaussian Process model valid for the Kiaman Superchron?, *J. Geophys. Res.: Solid Earth,* ***124,*** 6223-6242, doi:10.1029/2018JB016968

Panovska, S., C.G. Constable, & M. Korte, 2019. One hundred thousand years of geomagnetic field evolution, *Reviews of Geophysics,* ***57,*** doi:10.1029/2019RG000656

STEVEN CONSTABLE
Distinguished Professor

sconstable@ucsd.edu, marineemlab.ucsd.edu, 858-534-2409

Marine EM methods

Steven Constable heads the SIO Marine EM (Electromagnetic) Laboratory at IGPP. EM methods can be used to probe the geology of the seafloor, from the near surface to hundreds of kilometers deep, using electrical conductivity as a proxy for rock type. We have used these methods to study plate boundaries, marine gas hydrate, offshore geothermal prospects, permafrost, hydrothermal venting and associated massive sulfides, groundwater, and conventional oil and gas reservoirs.

During this past year we had a number of field campaigns. Our surface-towed shallow-water EM system was used o Hawaii to study offshore groundwater, in a project led by Eric Attias, a postdoc at the University of Hawaii. In collaboration with Jared Peacock of the USGS we collected land magnetotelluric (MT) data north of Mono Lake, following up on some results we obtained from lake-bottom data described in my 2017 annual report. PhD student Roslynn King used the surface-towed system o Santa Barbara to map tar seeps, and again o San Diego to look for offshore fresh groundwater (with success!). We had a month-long cruise out of Alaska collecting MT and EM data along the subduction zone, and collected MT sites across Spencer Gulf in South Australia.

In 2017 we recovered 38 MT instrument from the Mid-Atlantic Ridge (MAR), deployed a year earlier alongside an ocean-bottom seismic experiment. Postdoc Shunguo Wang has been working on this data set, in collaboration with our seismology colleagues at the University of Southampton. Figure 10 shows a result from this study, combining electrical resistivity, seismic velocity, and receiver function analysis. The agreement between the seismic and electrical methods is encouraging, with high conductivities,

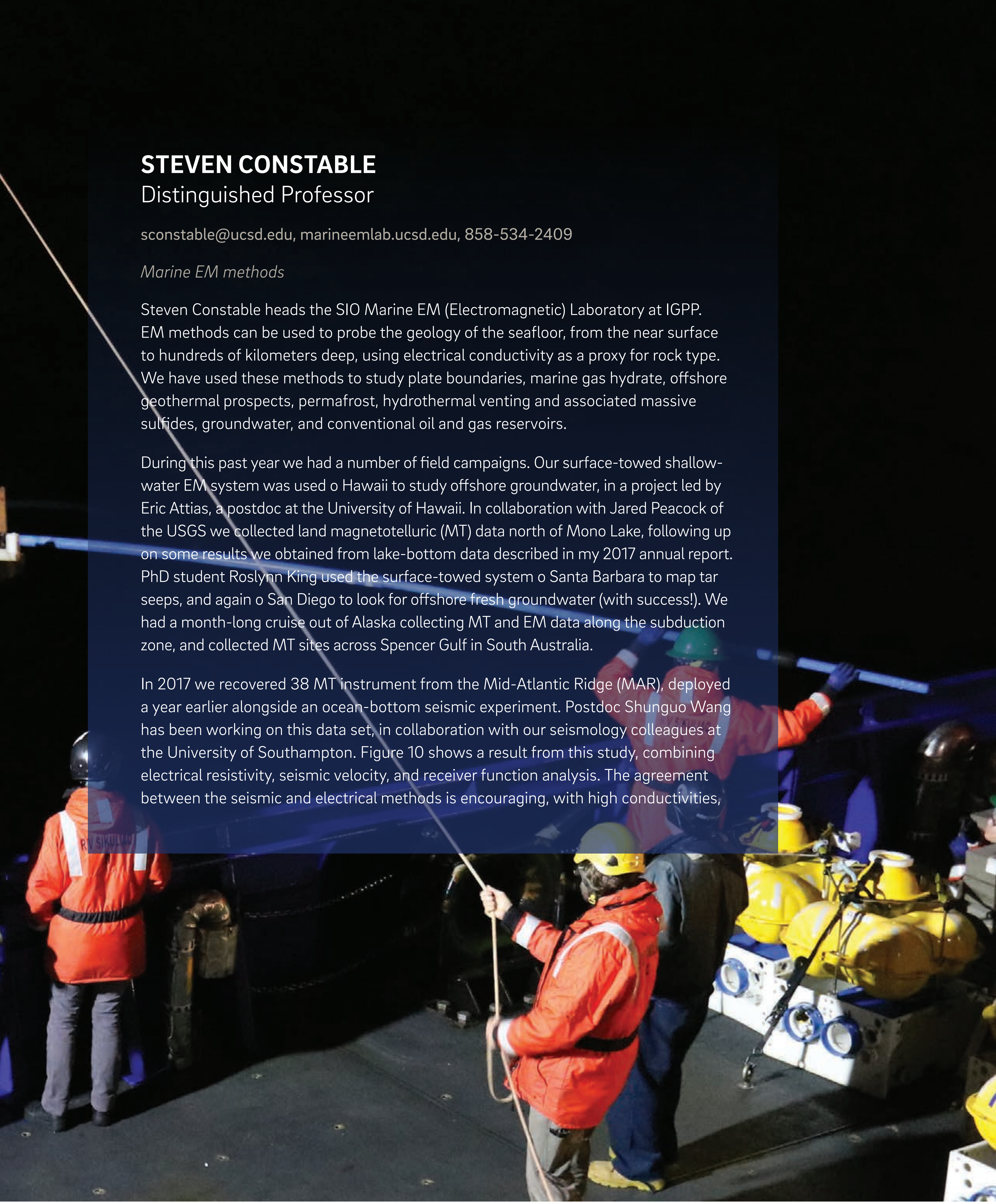

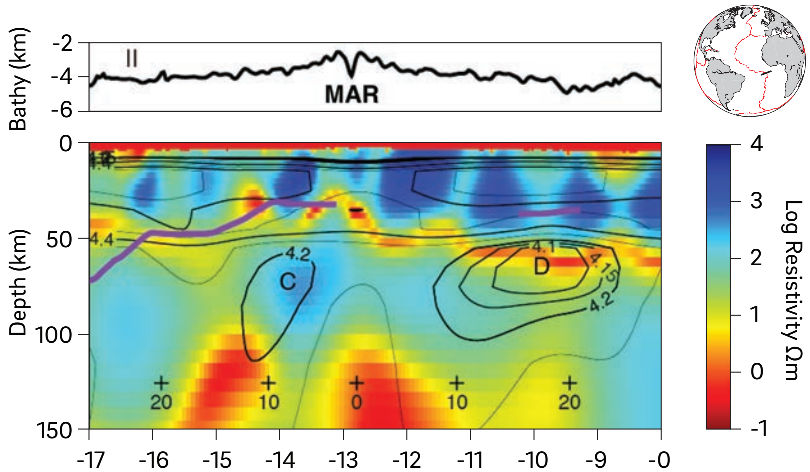

Figure 10. Composite geophysical model across the Mid-Atlantic Ridge (MAR), showing surface wave seismic velocity (black contours) overlain on electrical resistivity (color). Purple lines show negative polarity phases from S-to-P receiver functions. Modified from Rychert et al., manuscript in review.

and negative polarity phases coinciding to suggest a melt layer about 50 km deep at the lithosphere-asthenosphere boundary (LAB). This layer deepens with age away from the ridge, and is interpreted as upward melt migration in the mantle ponding beneath a freezing horizon.

We recently made progress analyzing an even older data set, collected in 2001 as part of the Anisotropy and Physics of the Pacific Lithosphere Experiment (APPLE). In this experiment we towed an EM transmitter in a 30 km radius circle around receiver instruments on 33 My old seafloor west of San Diego. The survey was designed specifically to detect anisotropy in the crust and upper mantle, which we did (Figure 11). In the crust, the direction parallel to the paleo-ridge axis is more conductive, consistent with cracking between dikes in the upper crust and faulting extending into the gabbroic lower crust, a result of normal faulting during extension and cracking during cooling. Below the Moho in the uppermost mantle, the conductive direction switches to the paleo-spreading direction, which we interpret as conduction between olivine grains in a mantle that has been sheared during plate formation.

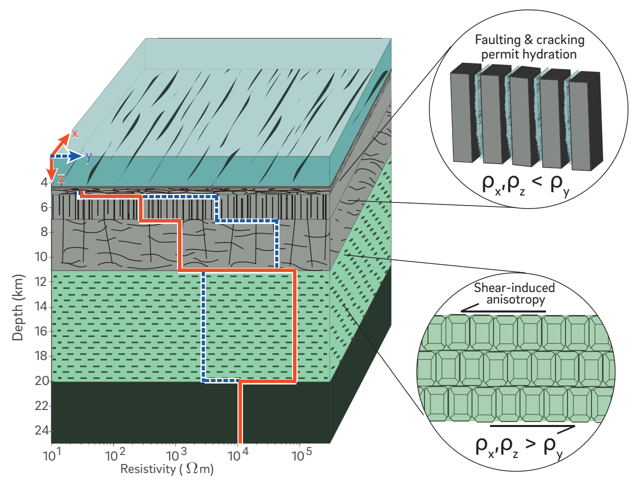

Figure 11. Electrical resistivity in the paleospreading direction (blue dashed line) and paleo ridge axis direction (red line), overlain on a schematic of a lithosphere with crustal cracking and sheared mantle. From Chesley et al., G-Cubed, accepted.

RECENT PUBLICATIONS

Constable, S., A. Orange, and D. Myer (2019): Marine CSEM of the Scarborough gas field, Part 3: Multicomponent 2D MT/CSEM inversions, *Geophysics*, ***84***, B387–B401. 10.1190/geo2019-0314.1

Cordoba-Ramırez, F., C.F. Luna, A. Gonzalez-Fernandez, S. Constable, J.G. Pena-Domınguez, E. Gomez-Trevino (2019): Marine controlled-source electromagnetics with geothermal purposes; central Gulf of California, Mexico, *Journal of Volcanology and Geothermal Research*, ***384***, 206–220. 10.1016/j.jvolgeores.2019.07.018

Wang, S., S. Constable, V. Reyes-Ortega, and C.A. Rychert (2019): A newly distinguished marine magnetotelluric coast effect sensitive to the lithosphere-asthenosphere boundary, *Geophysical Journal International*, ***218***, 978–987. 10.1093/gji/ggz202

Wang, S., M. Batani, S. Constable, T. Kalscheuer, and A. Malehmir (2019): Boat-towed radio-magnetotelluric and controlled-source audio-magnetotelluric study to resolve fracture zones at Aspo Hard Rock Laboratory site, *Sweden Geophysical Journal International*, ***218***, 1008–1031. 10.1093/gji/ggz162

Harmon, N., C. Rychert, M. Agius, S. Tharimena, T. Le Bas, J.M. Kendall, and S. Constable (2018): Marine geophysical investigation of the Chain Fracture Zone in the equatorial Atlantic from the PI-LAB experiment *Journal of Geophysical Research: Solid Earth* ***123***, 11,016–11,030. 10.1029/2018JB015982

J. PETER DAVIS
Specialist

pdavis@ucsd.edu, 858-534-2839

Seismology, time series analysis, geophysical data acquisition

My research responsibilities at IGPP center upon managing the scientific performance of Project IDA's portion of the IRIS/USGS Global Seismographic Network (GSN), a collection of 41 seismographic and geophysical data collection stations distributed among 29 countries worldwide. NSF recently renewed funding for an additional five years of GSN network operations via the IRIS Consortium.

To maintain the network in optimal working condition, IDA is in the process of replacing obsolete primary sensors with new models provided by our funding agency. Figure 12 shows one of these sensors being lowered into a 100m deep borehole to insure the quietest possible setting for recording distant earthquakes. Figure 13 shows results of some noise tests of a new vault sensor being conducted with our partners from the University of Stuttgart and the Karlsruhe Institute of Technology at their test facility in Germany's Black Forest.

Figure 12. IDA's Chris Sites and Clint Coon prepare to lower the new STS6A seismometer into the 100m deep borehole at station II.CMLA (Chã de Macela, Azores). Station operator Maria Escuer of our host organization, the OAC, assists. Photo courtesy C. Sites.

We are also installing infrasound sensors at several of our sites. In order to maximize data quality, we experimented with several types of spatial filters to suppress local wind noise. Figure 14 shows the test results of two such filters when they recorded signals created by the launch of the Mars InSight probe from nearby Vandenberg AFB. We expect to record infrasonic waves from a wide variety of phenomena using these instruments.

IDA staff members are working to fine-tune each station's instruments to enable scientists to extract the most accurate information possible from the data collected. One method for accomplishing this task is by examining key phenomena such as Earth tides and normal modes that should register the same on these important geophysical sensors. To the extent that measurements made with multiple instruments that have been calibrated in very different fashions match, we may have greater confidence that the instrument response information IDA distributes with GSN waveform data is accurate. Investigators use this information to compensate for the frequency-dependent sensitivity of sensors so that they may study true ground motion and its underlying physical causes.

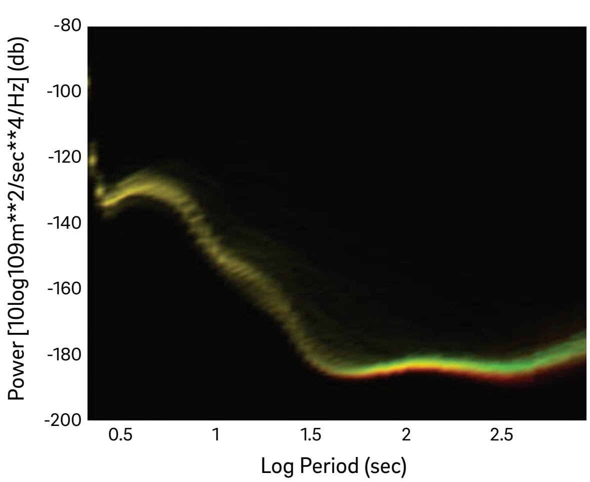

Figure 13. PSD noise estimates of two seismometers installed at BFO. Noise from one of the finest long period seismometers in the world, the STS1, is shown in red. Noise from a new model, the T360, is shown in green. Where the noise of the two overlaps appears in yellow. These results will factor into future development of the network.

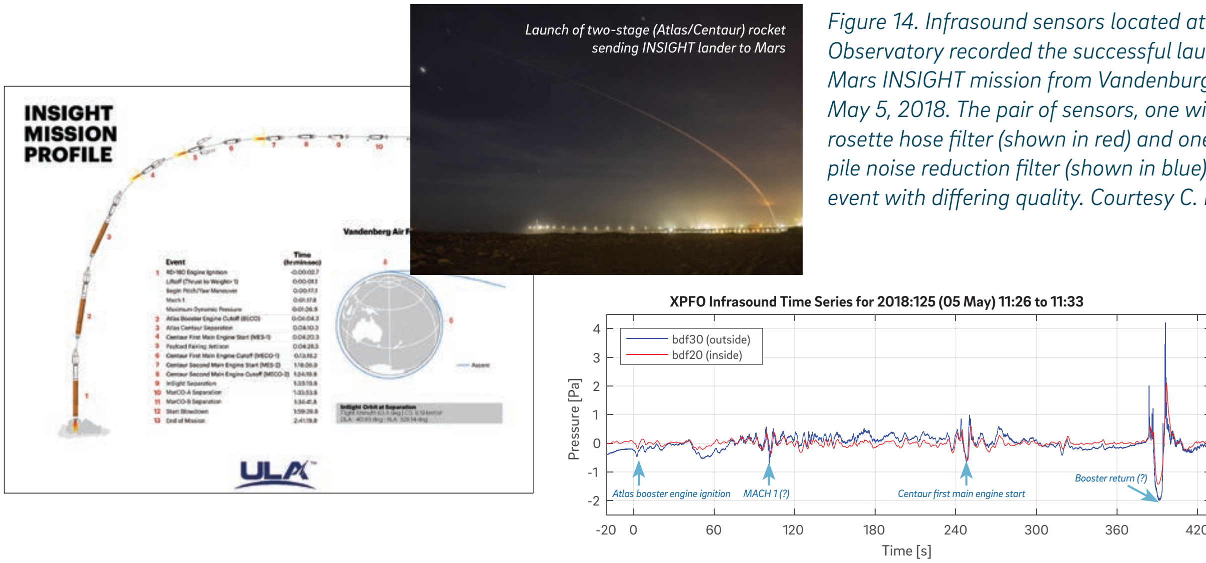

Figure 14. Infrasound sensors located at Pinyon Flat Observatory recorded the successful launch of the Mars INSIGHT mission from Vandenburg AFB on May 5, 2018. The pair of sensors, one with a flexible rosette hose filter (shown in red) and one with a rock pile noise reduction filter (shown in blue), recorded the event with differing quality. Courtesy C. Ebeling.

IDA is also playing a leading role in the GSN program by evaluating new models of seismometers that may be deployed within the GSN in the future such as the one whose performance is shown in Figure 13. IDA makes use of IGPP's Seismic Test Facility at Pinyon Flat Observatory to evaluate the behavior of instrument prototypes under conditions likely probe the limits of a sensor's capabilities. Pinyon Flat is quiet enough to permit the recording of faint signals from distant earthquakes but also experiences violent shaking from local events on nearby faults.

RECENT PUBLICATIONS

http://dx.doi.org/doi:10.7914/SN/II

http://dx.doi.org/doi:10.1785/0220170280

CATHERINE DE GROOT-HEDLIN

Research Scientist

chedlin@ucsd.edu; 858-534-2313

Acoustic propagation modeling with application to infrasound (sound at frequencies lower than human hearing); application of infrasound and seismic data to nuclear test-ban verification and hazard monitoring; use of seismic and infrasound networks to detect small-scale signals.

An automated event detector and locator: I have developed a 'Big Data' approach to detect and locate events in two-dimensional space and time using large volumes of data. This approach is called AELUMA (Automated Detection and Location of Events Using a Mesh of Arrays). AELUMA is used to create a catalog of infrasound sources in the eastern United States and southeastern Canada using infrasonic and seismic data recorded by large-scale networks. There are two main reasons to develop this catalog. First, the catalog provides a list of sources that can be used for basic infrasound research, either for remote study of the events themselves or to study of properties of the atmosphere. Second, we need to understand and document the noise field or other sources that may hamper the performance of International Monitoring System infrasound arrays in monitoring the Comprehensive Nuclear Test Ban Treaty.

Since its initial introduction to gravity data and infrasound data, the method has been expanded to include its application to seismic data, including both seismic surface waves and seismic body waves. The method has proven successful at finding small-scale signals in continental scale data sets, comprising several hundreds of seismic and infrasound stations. The detected signals include gravity waves caused by solar terminator waves observed in surface pressure, as well as gravity waves caused by convective storms. AELUMA has also been used to detect small

Figure 15. *Grey lines show groups of 3 stations (triads) used to estimate a bolide source location. Gray dots indicate infrasound stations where coherent signals were not detected; black dots mark where they were detected. Color-coding, at triads where coherent signals were detected show the signal arrival time in minutes after the start of 17 January 2018 (UTC). The arrows show the signal azimuth at each triad. The star marks the optimal source location in southwest Michigan. The error ellipse shows the range of acceptable locations.*

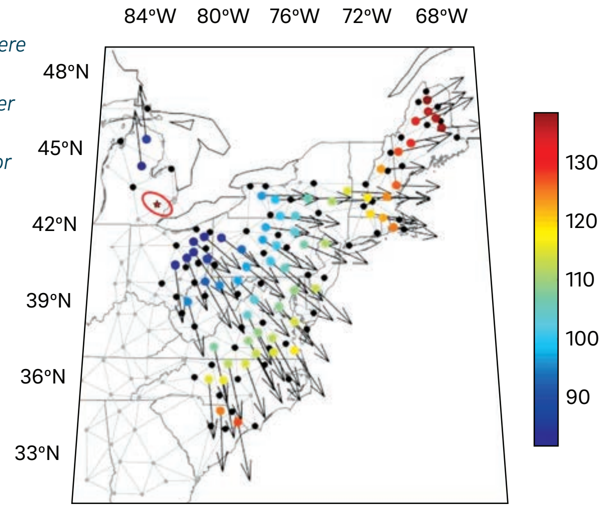

seismic events caused by fracking in Oklahoma detected by high frequency seismic data, and a bolide terminal burst over southeast Michigan, detected in infrasound data. Low frequency seismic surface wave data have been used to detect ice-quakes in Greenland, and most recently, stormquakes resulting from atmosphere-ocean-earth interaction during hurricanes or winter storms. A current project involves expanding the methodology to global data.

Numerical modeling: A basic research goal in infrasound is to understand the transmission of infrasound through variable atmospheric conditions. To this end, I developed a computationally efficient numerical method to synthesize the propagation of nonlinear acoustic waves through the atmosphere. Nonlinearity, or shock wave propagation, arises when pressure perturbations associated with acoustic waves are a significant fraction of the ambient atmospheric pressure. Shock waves are associated with meteoroid explosions in the upper atmosphere, volcanic eruptions, or nuclear and chemical explosions. Work on this code has progressed to allow for the incorporation of realistic atmospheric effects, such as spatially varying sound speeds and wind speeds, topography, and atmospheric attenuation. This code has been used to compute the penetration of sound into areas typically thought of as being in a "shadow zone", where sound refracts upwards, away from the Earth's surface due to the decrease in sound speed with altitude, much as light bends as it travels between air and water.

This code is now publicly available and has been used in several volcanology studies, including propagation of sound waves from volcanoes in Japan and Vanuatu.

RECENT PUBLICATIONS

de Groot-Hedlin, C., 2017, Infrasound propagation in tropospheric ducts and acoustic shadow zones, *J. Acoust. Soc. America*, ***142***, 1816-1827.

de Groot-Hedlin, C., Hedlin, M., L. Hoffmann M.J. Alexander, C. Stephan, 2017, Relationships between Gravity Waves Observed at Earth's Surface and in the Stratosphere over the Continental United States, J. *Geop. Res. – Atmos.*, doi.org /10.1002/2017JD027159.

de Groot-Hedlin, C.D., Hedlin, M.A.H. 2018, A New Automated Approach to Detecting and Locating Seismic Events Using Data from a Large Network. *Bull. Seis. Soc. Am.,* ***108:*** 2032–2045. doi: https://doi.org/10.1785/0120180072

de Groot-Hedlin, C.D., Hedlin, M.A.H. 2019, Detection of infrasound signals and sources using a dense seismic network, chapter in "Infrasound Monitoring for Atmospheric Studies," pp. 669-700.

Fan, W. JJ McGuire, CD. de Groot-Hedlin,, MAH. Hedlin, S. Coats, J. Fiedler. 2019, Stormquakes, *Geop. Res. Lett,* https://doi.org/ 10.1029/2019GL084217

Fan, W. C.D. de Groot-Hedlin,, M.A.H. Hedlin, Z. Ma. 2018, Using surface waves recorded by a large mesh of three-element arrays to detect and locate disparate seismic sources, *Geop. J. Int.,* https://doi.org/10.1093/gji/ggy316

Hedlin, M.A.H., J. Ritsema, C.D. de Groot-Hedlin, E.A. Hetland, 2018, A Multidisciplinary Study of the 17 January 2018 Bolide Terminal Burst over Southeast Michigan. *Seis. Res. Lett.* doi: https://doi.org/10.1785/0220180157

Hedlin, M.A.H., C.D. de Groot-Hedlin, J.M. Forbes, D.P. Drob, Solar Terminator Waves in Surface Pressure Observations, *Geop. Res. Lett,* https://doi.org/10.1029/2018GL078528

MATTHEW DZIECIUCH
Research Geophysicist

mdzieciuch@ucsd.edu; 858-534-7986

Acoustical oceanography, ocean acoustic tomography, signal processing

Low-frequency, long-range ocean acoustics experiments provide a wealth of knowledge about an otherwise opaque underwater environment. The travel-time of sound waves propagating through the depths is affected by both small-scale and large-scale ocean processes. Acoustical oceanography seeks to use sound propagation in the ocean to understand some of the dynamic processes that are present.

Sound is an effective tool to study the ocean interior because it is trapped in a natural occurring waveguide (due to vertical gradients of pressure and temperature) present in all the worlds oceans. Some of the processes that can be studied include climate change, ocean circulation, internal waves, and tides. I am part of a group that has conducted several large experiments in regions as diverse as the Philippine Sea in the tropical Pacific, to the Beaufort Sea in the Arctic.

This past year we have deployed moorings for a new experimental program in the Arctic that would measure the heat content along a trans-Arctic path extending from near Svalbard to near the North Slope of Alaska. A map of the 2019 deployment is shown in Figure 16. Part of the motivation is to repeat a measurement done 25 years ago by Mikhalevsky et al. in order to see how much the acoustic propagation (and by inference, the heat content) has changed.

A second motivation is that the acoustic equipment has much improved in the past 25 years and thus we will be able to obtain much finer detailed measurements. Increased source efficiency allows us to produce a year long time-series from fixed moorings rather than a few transmissions from a drifting ice camp. Furthermore, advances in storage and clocks allows for a much denser sampling of the acoustic field with 40 element vertical line arrays and an accurate time base produces meaningful acoustic travel-times.

The sound source operates near 35 Hz in order to avoid the rough ice-cover scattering losses associated with higher frequencies. The stratification of the Arctic is complicated and has been changing rapidly in past few years. Above the deep Arctic water, there is the warm, salty Atlantic layer, the less salty but cold Pacific winter water, then the warmer Pacific summer water, while on top is fresher but cold water either from the melting ice or from the large amount of river in flows. The composition and thicknesses of these layers have been greatly affected by climate change and thus acoustic propagation

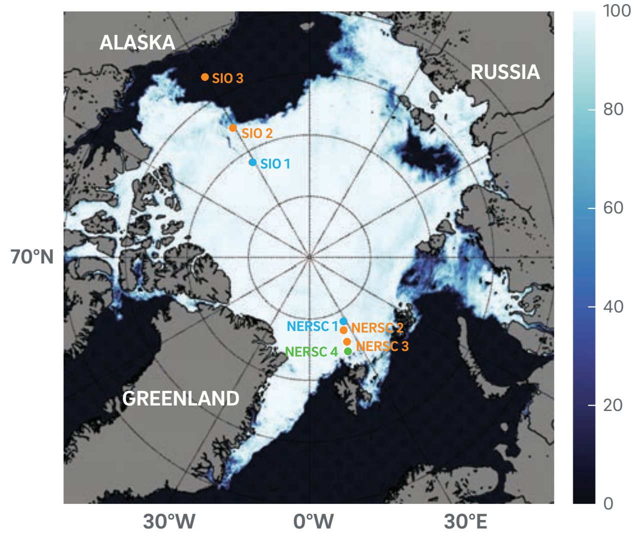

Figure 16. Deployed experimental layout of the CAATEX field program. The blue dots designate acoustic transceivers (sources and vertical line arrays.) While the orange dots designate acoustic receivers only.

through these layers has also been affected. The experiment has been designed to learn the most possible from the acoustic travel-time, transmission loss, and scattering loss as the sound interacts with the stratification and with the rough ice-cover.

The field program will collect data for one year and then be recovered in 2020. This experiment is being conducted with funding from the Office of Naval Research, they have supported CAATEX as well as previously deployed experiments, to further our ability to monitor and understand the changing Arctic.

RECENT PUBLICATIONS

Skarsoulis, E.K., Cornuelle, B.D., Dzieciuch, M.A., (2009) Travel-time sensitivity kernels in long-range propagation, *J. Acoust. Soc. Am.,* ***126,*** 2223{2233.

Dzieciuch, M.A., Signal processing and tracking of arrivals in ocean acoustic tomography, (2014) *J. Acoust. Soc. Am.,* ***136,*** 2512{2522.

Sagen, H., Geyer, F., Sandven, S., Babiker, M., Dushaw, B., Worcester, P., Dzieciuch, M., and Cornuelle, B., (2017) Resolution, identication, and stability of broadband acoustic arrivals in Fram Strait, *J. Acoust. Soc. Am.,* ***141,*** 2055{2068.

Ozanich, E., Gerstoft, P., Worcester, P., Dzieciuch, M., and Thode, A., (2017) Eastern Arctic ambient noise on a drifting vertical array, *J. Acoust. Soc. Am.,* ***142,*** 1997{2006.

YURI FIALKO

Professor

yfialko@ucsd.edu; 858-822-5028

Earthquake physics, crustal deformation, space geodesy, volcanology

Professor Fialko's research is focused on understanding the mechanics of seismogenic faults and magma migration in the Earth's crust, through application of principles of continuum and fracture mechanics to earthquakes and volcanic phenomena. Prof. Fialko is using observations from space-borne radar satellites and the Global Positioning System (GPS) to investigate how the Earth's crust responds to seismic and magmatic loading.

One of the long-term research interests of Prof. Fialko is deformation due to active faults in Southern California. Southern California hosts a number of active faults, including major plate boundary faults such as the San Andreas fault, a mature strike-slip fault capable of great earthquakes. The southern section of the San Andreas fault (SSAF) has not produced a large earthquake in the last 300 years and is believed to be in the late inter-seismic stage of the earthquake cycle. The SSAF is also known to creep in the top few kilometers of the upper crust. An average creep rate on the SSAF is 2-4 mm/yr, based on creepmeter measurements, and offsets of man-made structures and well-dated geologic features corresponding to time intervals of several years to a few hundred years. Instrumental measurements of surface creep on the SSAF, however, indicate that the creep is not steady and is punctuated by episodes of

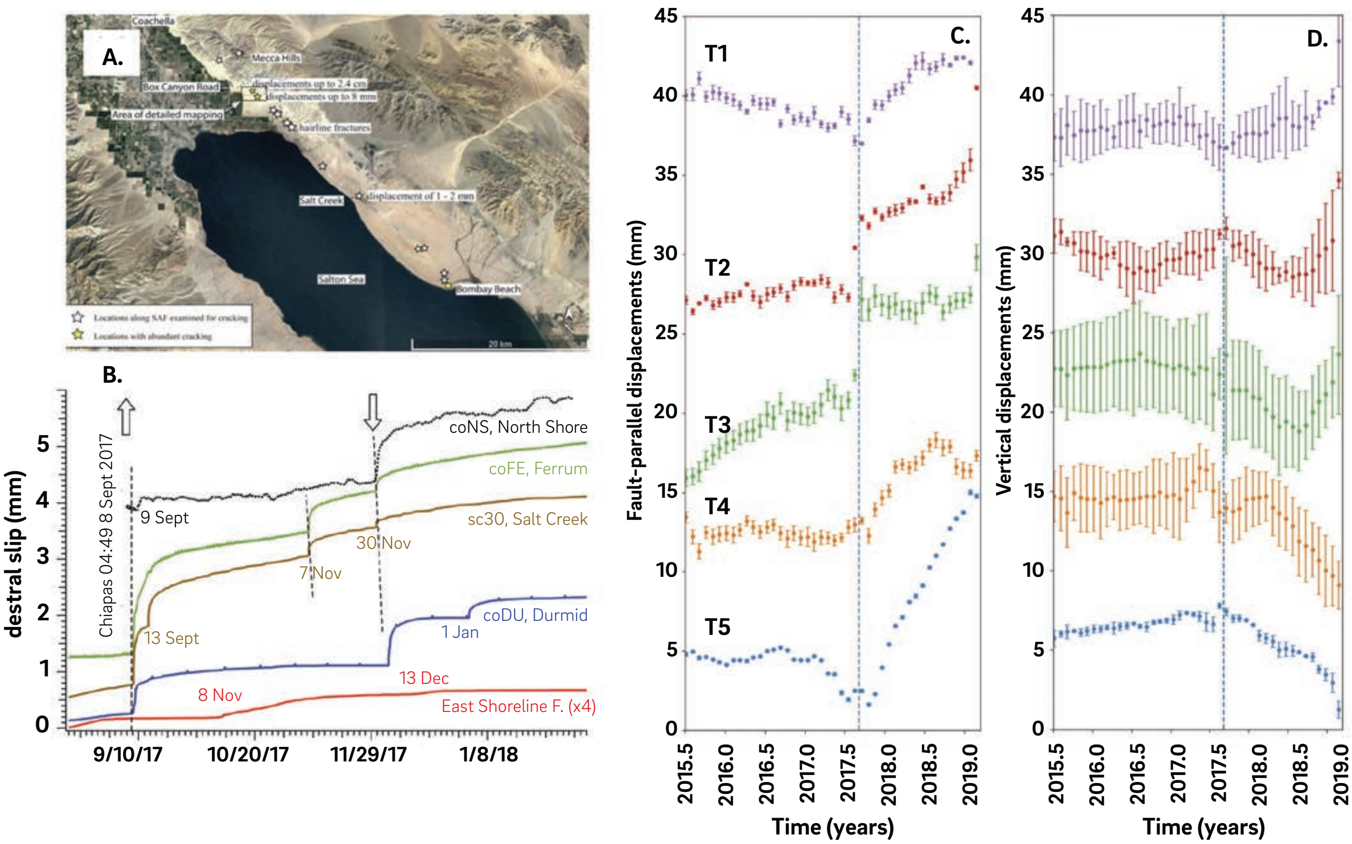

Figure 17: Observations of slow slip event on the SSAF triggered by the 2017 Chiapas (Mexico) d slip was investigated during a field survey in January of 2018. Notable surface cracks with measurable offsets were found in the \area of detailed mapping" (yellow stars). b) Fault slip recorded by creepmeters at several locations along the SSAF. The Chiapas earthquake initiated rapid slip within minutes of the earthquake, followed by several subevents (marked by short vertical dashed lines). c, d) Time series of fault-parallel (c) and vertical (d) displacements, along with uncertainties, derived from Sentinel-1 InSAR data from different lines of sight. The dashed vertical line denotes the time of the Chiapas earthquake. From Tymofyeyeva et al. (2019).

accelerated slip that can last days to months. In order to better understand the time dependence and the mechanisms of shallow creep, Prof. Fialko and a former graduate student Katia Tymofyeyeva (now a researcher at JPL/Caltech) used Interferometric Synthetic Aperture Radar (InSAR) data from the Sentinel-1 mission to map surface deformation along the SSAF. Data from the ascending and descending satellite orbits were combined to obtain horizontal and vertical components of the surface displacement field. The time series of surface displacements revealed that creep on the SSAF has considerably accelerated compared to the long-term average starting in September of 2017 (Figure 17c). The InSAR data were confirmed by creepmeter measurements and geologic observations of surface cracking along the fault trace (Figure 17 a,b). The onset of accelerated creep coincides with the time of the 2017 M8.2 Chiapas (Mexico) earthquake that occurred 3000 km away, implying dynamic triggering. The extremely low triggering stress, on the order of 10 kPa, implies extraordinary sensitivity of the shallow fault zone and yet much larger stress perturbations, e.g., during the 2010 El-Mayor Cucapah earthquake (on the order of 1 MPa) have not triggered a much larger slip compared to the 2017 event. A 2D fault zone model assuming monotonic variations in the velocity-dependence parameter (a - b) is able to reproduce a number of features in the observed slip histories. However, more complicated models including e.g. stochastic variations in the rate and state parameters, or rate-dependent hardening mechanisms such as dilatancy, may be required to fit all of the available data.

In another recent study Prof. Fialko and a former graduate student Kang Wang (now a post-doc at UC Berkeley) investigated how the Tibetan lithosphere responded to the 2015 Mw 7.8 Gorkha (Nepal) earthquake that occurred along the central Himalayan arc. This study involved analysis of space geodetic observations including InSAR data from Sentinel-1A/B and ALOS-2 satellites, as well as GPS data from a local network. InSAR observations revealed an uplift of up to 35 70 mm over 35 20 months after the mainshock, concentrated primarily at the downdip edge of the ruptured asperity. This is in agreement with the GPS observations that also show uplift, as well as southward movement in the epicentral area, qualitatively similar to the co-seismic deformation pattern. Kinematic inversions of GPS and InSAR data, and forward models of stress-driven creep suggest that the observed post-seismic transient is dominated by afterslip on a down-dip extension of the seismic rupture. All tested visco-elastic models predict opposite signs of horizontal and vertical displacements compared to those observed. Available surface deformation data therefore appear to rule out a hypothesis of a low viscosity channel beneath the Tibetan Plateau which has been previously invoked to explain the long-term uplift and variations in topography at the plateau margins.

RECENT PUBLICATIONS

Tymofyeyeva, E., Y. Fialko, et al., Slow slip event on the southern San Andreas fault triggered by the 2017 Mw8.2 Chiapas (Mexico) earthquake, *J. Geophys. Res.,* ***124***, 9956-9975, 2019.

Wang, K. and Y. Fialko, Observations and modeling of co- and post-seismic deformation due to the 2015 Mw 7.8 Gorkha (Nepal) earthquake, *J. Geophys. Res.,* ***123,*** 761-779, 2018.

HELEN AMANDA FRICKER

Professor, John Dove Isaacs Chair

hafricker@ucsd.edu; 858-534-6145, polar.ucsd.edu

Cryosphere, Antarctic ice sheet, subglacial lakes, ice shelves, satellite remote sensing

We are located in MESOM with OA Prof Fiamma Straneo, forming the core of the Scripps Polar Center. I am a member of NASA's ICESat-2 Science Team. I became an AGU Fellow in December 2017. I am an Honorary Professor at University of Swansea starting 1 February 2020.

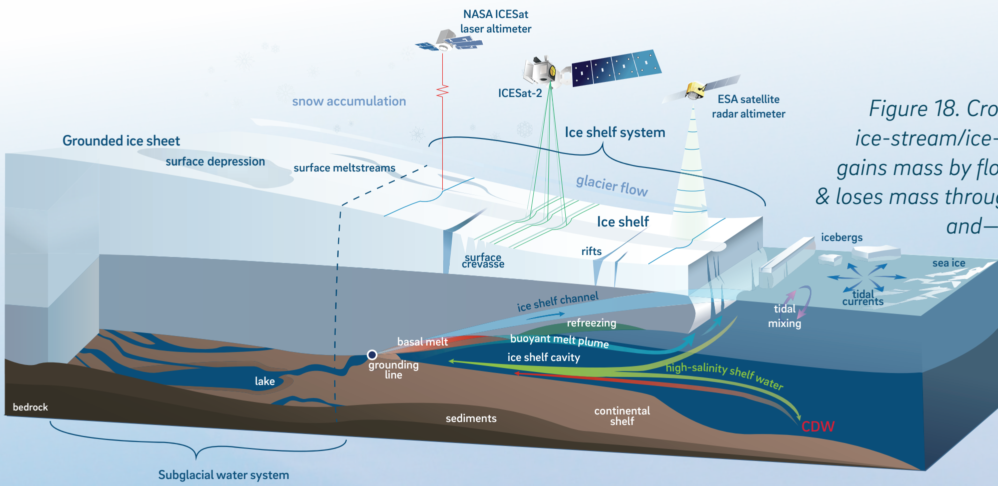

Figure 18. Cross-section of a typical Antarctic ice-stream/ice-shelf system. Ice-shelf system: Ice gains mass by flow of grounded ice & local snowfall, & loses mass through iceberg calving, basal melting and—to a lesser degree—surface melting. In some regions, warm circum-polar deep water flows into the sub-ice cavity. Subglacial water system: Active subglacial lakes modulate water flow through the subglacial water system, water that discharges into the sub-ice cavity, enhancing basal melt rates.

My research focuses on understanding the processes driving changes on the Antarctic ice sheet. One of the main unknowns is Antarctica's current contribution to global sea level rise, & predicting how that will change in the future. Because Antarctica is so large, & the time scales on which it changes are so long (decades to centuries), the only viable way to monitor it is with satellites. The main technique we use is satellite altimetry (radar altimetry from ESA's ERS-1/ERS-2/Envisat (1994-2012) or laser altimetry from NASA's Ice, Cloud & land Elevation Satellite (ICESat 2003-2009) & ICESat-2 (launched 15 Sept 2018)); these multiple missions have provided ice sheet height data for ~25 years. Using the long, continuous altimeter records we can learn about the processes that are leading to accelerated mass loss. **We focus mainly on two key dynamic components of the Antarctic ice-sheet system: (i) floating ice shelves & (ii) active subglacial lakes (Figure 18).**

Ice shelves: ice shelves surround Antarctica & are where most of the mass loss takes place. Since ice shelves are floating, their melting does not contribute directly to sea level. However, ice shelves provide mechanical support to 'buttress' seaward flow of grounded ice, so that ice-shelf thinning & retreat result in enhanced ice discharge across the grounding line (GL) to the ocean. Our group specializes in monitoring Antarctic ice shelves from satellite altimetry (radar & laser). Funded by NASA, we generate estimates of ice-shelf surface height continuously since the early 1990s & use these to understand the mass loss processes from ice shelves. These data revealed accelerated losses in total Antarctic ice-shelf volume from 1994 to 2012. In East Antarctica, the first half of the record showed a mass increase, likely a result of increased accumulation. In West Antarctica, in particular the Bellingshausen & Amundsen Sea regions, ice shelves lost mass throughout the record with changes on multi-year time scales. Ice-shelf thinning in these regions was substantial (some ice shelves thinned 18% in 18 years), raising concerns about future loss of grounded ice & resulting sea level. GP student Susheel Adusumilli generated updated time series for 1994 to 2018 & estimated basal melt rates for all ice shelves; this work is in revision at Nature Geoscience.

I was a PI on an NSF project ROSETTA-Ice to investigate the Ross Ice Shelf using airborne geophysics (gravity, laser & radar). GP student Maya Becker participated in the 2016/2017 & 2017/2018 field seasons & is comparing those data with ICESat & ICESat-2 data, to investigate ice shelf mass balance processes (ice fronts & marine ice). Postdoc Cyrille Mosbeux is an ice-sheet modeler looking at how the grounded ice responds to changes in the ice shelf.

Subglacial lakes: In 2006, I discovered active subglacial water systems under the fast-flowing ice streams of Antarctica in repeat-track ICESat data; O(m) height changes corresponded to draining & filling of subglacial lakes. We continue to monitor active lakes & have found 124 in total throughout Antarctica. I was PI on an interdisciplinary 6-year NSF project WISSARD which drilled in Jan 2013 into Whillans Subglacial Lake on Whillans Ice Stream & the region of the GL across which the subglacial water flows & enters the ocean. Mercer Subglacial Lake was drilled during the NSF-funded 5-year project Subglacial Antarctic Lakes Scientific Access (SALSA) in Jan 2018 & Matt Siegfried (former SIO student) led the geophysics team, which also included former IGPP Prof. Kerry Key & GSR Chloe Gustafson in 2018 who made EM measurements, and 2nd year student Philipp Arndt in 2019.

RECENT PUBLICATIONS

Smith, B., H. A. Fricker, A. S. Gardner, B. Medley, J. Nilsson, F. S. Paolo, N. Holschuh, S. Adusumilli, K. Brunt, B. Csatho, K. Harbeck, T. Markus, T. Neumann, M. R. Siegfried, H. J. Zwally Pervasive ice sheet mass loss reflects competing ocean and atmosphere processes, accepted to *Science,* January 2020.

Das, I., L. Padman, R. E. Bell, H. A. Fricker, K. J. Tinto, C. L. Hulbe, C. S. Siddoway, T. Dhakal, N.P. Frearson, C. Mosbeux, S. I. Cordero, M. R. Siegfried (2020) Multi-decadal basal melt rates & structure of the Ross Ice Shelf, Antarctica from airborne ice penetrating radar, *Journal of Geophysical Research,* in press.

Smith, B., H. A. Fricker, A. S. Gardner, B. Medley, J. Nilsson, F. S. Paolo, N. Holschuh, S. Adusumilli, K. Brunt, B. Csatho, K. Harbeck, T. Markus, T. Neumann, M. R. Siegfried, H. J. Zwally (2020) Pervasive ice sheet mass loss driven by competing ocean & atmosphere processes, *Science,* in press.

Gudmundsson, G. H., F. S. Paolo, S. Adusumilli, H. A. Fricker (2019). Instantaneous Antarctic ice sheet mass loss driven by thinning ice shelves. *Geophysical Research Letters,* ***46***(23), 13903-13909.

Smith, B., H.A. Fricker, N. Holschuh, A.S. Gardner, S. Adusumilli, K.M. Brunt, B. Csatho, K. Harbeck, A. Huth, T. Neumann, J. Nilsson, M. R. Siegfried (2019) Land ice height-retrieval algorithm for NASA's ICESat-2 photon-counting laser altimeter, Remote Sensing of the Environment, *Remote Sensing of the Environment,* https://doi.org/10.1016/j.rse.2019.111352.

Porter, D. F, S. R. Springer, L. Padman, H.A. Fricker, K. J. Tinto, S. C. Riser, R. E. Bell, & the ROSETTA-Ice Team (2019) Evolution of the seasonal surface mixed layer of the Ross Sea, Antarctica, observed with autonomous profiling floats, *Journal of Geophysical Research-Oceans,* doi: 10.1029/2018JC014683.

Tinto, K., Padman, L., Siddoway, C.S., Springer, S.R., Fricker, H.A., Das, I., Caratori Tontini, F., Porter, D.F., Frearson, N.P., Howard, S., Siegfried, M.R., Mosbeux, C., Becker, M., Bertinato, C., Boghosian, A., Brady, N., Burton, B.L., Chu, W., Cordero, S.I., Dhakal, T., Dong, L., Gustafson, C.D., Keeshin, S., Locke, C., Lockett, A., O'Brien, G., Spergel, J.J., Starke, S.E., Tankersley, M., Wearing, M., Bell, R.E. (2019) Ross Ice Shelf response to climate driven by tectonic imprint on seafloor bathymetry, *Nature Geoscience,* https://doi.org/10.1038/s41561-019-0370-2.

Borsa, A.A., H.A. Fricker, K.M. Brunt (2019) A terrestrial validation of ICESat elevation measurements, *IEEE Transactions on Geoscience and Remote Sensing,* ***15***(9), doi: 10.1109/TGRS.2019.2909739.

MICHAEL A.H. HEDLIN

Research Geophysicist

hedlin@ucsd.edu; 858-534-8773

Study of large atmospheric phenomena, study of long-range propagation of subaudible sound in the atmosphere, seismo-acoustics

INFRASOUND: The study of subaudible sound, or infrasound, has emerged as a new frontier in geophysics and acoustics. We have known of infrasound since 1883 with the eruption of Krakatoa, as signals from that event registered on barometers around the globe. Initially a scientific curiosity, the field briefly rose to prominence during the 1950's and 1960's during the age of atmospheric nuclear testing. With the recent Comprehensive Test-Ban Treaty, which bans nuclear tests of all yields in all environments, we have seen renewed interest in infrasound. A worldwide network of infrasound arrays, being constructed for nuclear monitoring, is fueling basic research into man-made and natural sources of infrasound, how sound propagates through our dynamic atmosphere and how best to detect infrasonic signals amid noise due to atmospheric circulation. This network has been supplemented with deployments, such as the 400-station seismo-acoustic USArray Transportable Array (TA), for basic research and enhanced monitoring of regions of great interest.

RESEARCH AT L2A: The Laboratory for Atmospheric Acoustics (L2A) is the home of research in this field at IGPP. Several faculty, post-docs and PhD students work full or part time in L2A, supported by engineers and technicians in the lab and the field. More information about this lab can be found at l2a.ucsd.edu. Presently we study a broad suite of problems related to both natural and man-made sources.

DENSE NETWORK STUDIES: The global infrasound network is unprecedented in scale however it is still very sparse, with ~ 100 stations operating worldwide. To increase the density of sampling of the infrasonic wavefield we have used acoustic–to-seismic coupled signals recorded by dense networks, such as the 400-station USArray Transportable Array (TA) and various PASSCAL deployments. We have used the original (seismic-only) TA network to create a catalog of atmospheric events in the western United States similar to commonly used seismic event catalogs. The acoustic

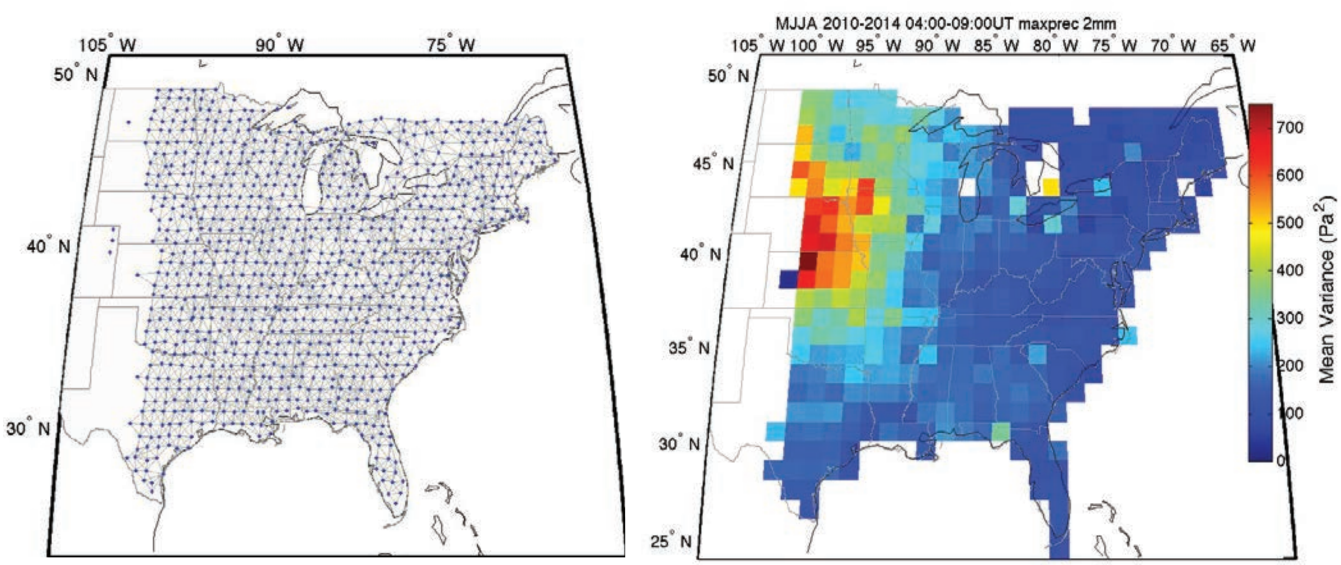

Figure 19: (left) sites occupied by stations in the TA from January 1, 2010 through Sept 30, 2014. These stations have been grouped into 3-element arrays (triads) for the study of long-period atmospheric gravity waves. The panel on the right shows the variance of atmospheric pressure in the 2-6 hr passband during the thunderstorm seasons from 2010 through 2014. The high variance near the Great Lakes is due to gravity waves excited by convective storms.

catalog is used in part to find sources of interest for further study and to use the recorded signals to study long-range infrasound propagation. Recorded signals from instantaneous sources are commonly dispersed in time to several 10's of seconds. Modeling indicates that this is due to interaction of the sound waves with fine-scale structure in the atmosphere due to gravity waves. We are currently using infrasound to constrain the statistics of this time-varying structure.

The National Science Foundation funded our group to upgrade the entire TA with infrasound microphones and barometers. Our sensor package is sensitive to air pressure variations from D.C. to 20 Hz, at the lower end of the audible range. The upgrade converted the TA into the first-ever semi-continental-scale seismo-acoustic network. The network has moved east across the US as stations are redeployed. Figure 19 (left panel) shows station locations from January 1, 2010 through the end of September, 2014. We have divided this collection of stations into 3,600 elemental arrays (triads) to study atmospheric gravity waves. An early result is shown in the right panel of Figure 18. This map shows the variance of atmospheric pressure in the 2-6 hour pass-band at local night. Elevated variance of atmospheric pressure is due to the presence of atmospheric gravity waves. As expected, large gravity waves are common to the west of the Great Lakes and are from convective activity.

FIELD OPERATIONS: Our group has built infrasound arrays for nuclear monitoring in the US and Africa. We operate research arrays located near San Diego.

RECENT PUBLICATIONS

Brown, P., Assink, J., Astiz, L.,Blaauw, R., Boslough, M., Borovicka, J., Brachet, N., Brown, D., Campbell-Brown, M., Ceranna, L., Cooke, W., de Groot-Hedlin, C., Drob, D., Edwards, W. Evers, L., Garces, M., Gill, J., Hedlin, M.A.H., Kingery, A., Laske, G., Le Pichon, A., Mialle, P., Moser, D., Saffer, A., Silber, E., Smets, P., Spalding, R., Spurny, P., Tagliaferri, E., Uren, D., Weryk, R., Whitaker, R., Krzeminski, Z., 2013, The Chelyabinsk airburst: Implications for the Impact Hazard, *Nature*, DOI: 10.1038/nature12741.

de Groot-Hedlin, C.D., Hedlin, M.A.H., Hoffmann, L., Alexander, M.J. and Stephan, C., 2017, Relationships between Gravity Waves Observed at the Surface and in the Stratosphere over the Continental United States, *JGR Atmospheres,* DOI: 10.1002/2017JD027159.

Fan, W., de Groot-Hedlin, C.D., Hedlin, M.A.H. and Ma, Z., 2018, Using surface waves recorded by a large mesh of three-element arrays to detect and locate disparate seismic sources, *Geophysical Journal International,* ***215,*** p942-958, https://doi.org/10.1093/gji/ggy316

Fan, W., McGuire, J.J., de Groot-Hedlin, C.D., Hedlin, M.A.H., Coats, S. and Fiedler, J.W. 2019, Stormquakes, *Geophysical Research Letters,* doi: 10.1029/2019GL084217

Hedlin, M.A.H. and Drob, D.P., 2014, Statistical characterization of atmospheric gravity waves by seismoacoustic observations, *J. Geophys. Res. Atmos.,* doi: 10.1002/2013JD021304.

Hedlin, M.A.H., de Groot-Hedlin, C.D., Forbes, J. and Drob, D., 2018, Solar Terminator Waves in Surface Pressure Observations, *Geophysical Research Letters,* ***45,*** DOI:10.1029/2018GL078528.

Hedlin, M.A.H., de Groot-Hedlin, C.D., Ritsema, J., Hetland, E., 2018, A multidisciplinary study of the January 17, 2018 bolide terminal burst over southeast Michigan, *Seismological Research Letters,* ***89*** (6): 2183-2192, https://doi.org/10.1785/0220180157.

DEBORAH LYMAN KILB

Project Scientist

dkilb@ucsd.edu; eqinfo.ucsd.edu/~dkilb/current; 858-822-4607

Research Interests: Crustal seismology, earthquake early warning and earthquake triggering. Diversity Interests: Improving how science is communicated to students and the public. Placing an importance on promoting jobs requiring skills within the intersection of science and art. Cultivating diversity within our communities.

Icequakes and glacier surface crevassing [Garcia et al., 2019]. Using seismology and geodesy in tandem, we explore the behavior of surface crevassing and icequakes near a seasonal glacier-dammed lake at Gornergletscher, Switzerland. This lake experiences outburst floods annually in midsummer. To study the interplay between lake drainage, glacier movement and crevasse activity, we use high-frequency seismic data and geodetic data from networks deployed near the lake during three summers (2004, 2006 and 2007). We use a Rayleigh wave coherence method to locate ~15,000 icequakes that primarily map well-defined surface crevasses, and we compute 2D strains from triads of GPS stations. We find crevasse icequake activity and glacial velocity are highest in the early season, then decrease as meltwater channels erode and subglacial water pressure decreases (Figure 20). Glacial response to lake drainage varied year-to-year, with icequake activity promoted at some crevasses and inhibited at others, suggesting icequakes may be indicative of local drainage patterns and small-scale features of the stress field. Diurnal pulses in icequake activity exhibit peak activity at different times of day in different locations, coincident with a southeast-to-northwest trending concentrated shear zone near the Gornergletscher–Grenzgletscher confluence, which we attribute to differences in the timing of peak strain rates in these regions.

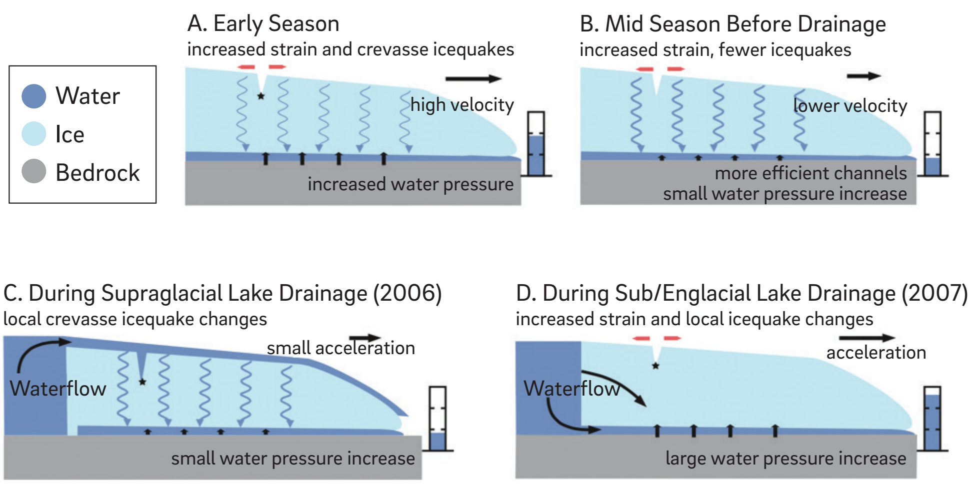

Figure 20. Cartoon cross-section of the glacier (light blue), lake water (dark blue) and glacier bed (gray). This schematic shows the proposed relationship between meltwater, icequake activity and glacial motion during (a) early season, (b) middle season prior to lake drainage, (c) supraglacial drainage in 2006 and (d) subglacial and englacial drainage in 2007. Surface icequakes are depicted as crevasse openings in regions of strain increases (red arrows). Black horizontal arrows indicate glacier motion. Wavy blue arrows indicate water percolation to the glacier base, and vertical black arrows and adjacent standpipes indicate basal water pressure increase. Water flow directions during lake drainage are also shown.

Earthquake early warning in southern California [Cochran et al., 2019]. We test the Japanese ground-motion-based earthquake early warning (EEW) algorithm "propagation of local undamped motion (PLUM)," using southern California data. Unlike most EEW systems that use source-based methods that estimate the location, magnitude, and origin time of an earthquake, and, in turn use ground-motion prediction equations to identify regions of expected strong shaking, the PLUM algorithm simply uses observed ground motions directly to define alert areas. We assess PLUM using (a) a dataset of 193 magnitude 3.5+ southern California earthquakes (2012-2017), and (b) a suite of testing and certification data that includes 49 earthquakes in addition to other seismic signals. The latter includes events that challenge current

EEW algorithms. Exploring different alerting thresholds, we find the optimal configuration is a two-station method using modified Mercalli intensity (MMI) thresholds of 4.0 and 2.5 for the first and second stations, respectively. PLUM successfully detected 12 of 13 magnitude 5.0+ earthquakes (e.g., Figure 21) and issued no false alerts. PLUM alert latencies were similar to, and, in some cases faster, than the source-based algorithms. This can net a reduction in the areal extent of the 'blind zone' where no warning can be issued near the earthquake. PLUM is a simple, independent seismic method that may complement existing source-based algorithms in EEW.

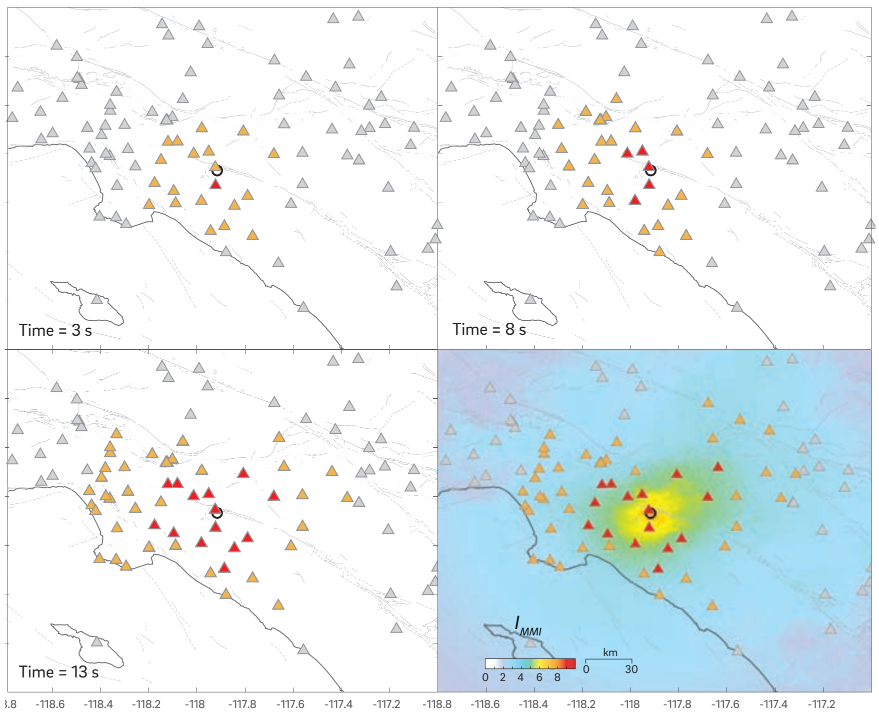

Figure 21. Evolution of the PLUM alert area for the 2014 magnitude 5.1 La Habra earthquake (open circle). Triggered stations (red triangles) and those predicted to exceed the threshold (orange triangles) at 3, 8, and 13 s after the event origin time. The first alert is issued 3 seconds after the earthquake origin time, and the alert area grows as more stations exceed the thresholds. The final distribution of stations that exceeded the threshold (red) and those predicted to exceed the threshold (orange) are juxtaposed on the USGS ShakeMap (lower right). Note that all stations that PLUM predicted to exceed the MMI=4 threshold, but were not exceeded on the ShakeMap, are within 30 km of a station that did exceed the threshold. This zone of over-alerting (e.g., locations where ground motions are predicted to exceed the threshold but do not) is inherent to PLUM.

RECENT PUBLICATIONS

Cochran, E. S., J. Bunn, S.E. Minson, A.S. Baltay, D. Kilb, Y. Kodera and M. Hoshiba [2019]. Event detection performance of the PLUM earthquake early warning algorithm in Southern California. *Bull. Seism. Soc. Am.*, doi: 10.1785/0120180326.

Garcia*, L., K. Luttrell, D. Kilb and F. Walter [2019]. Joint geodetic and seismic analysis of surface crevassing near a seasonal glacier-dammed lake at Gornergletscher, Switzerland. *Annals of Glaciology*, 1-13. doi: 10.1017/aog.2018.32.

Kilb D., A. Yang, N. Garrett**, K. Pankow, J. Rubinstein and L. Linville [2018]. "Tilt trivia: a free multiplayer app to learn geoscience concepts and definitions", *Seismological Research Letters, **89***: 1908-1915. https://doi.org/10.1785/0220180049. http://siogames.ucsd.edu/TiltTrivia/index.html

Linville* L.M., K. L. Pankow and D. Kilb [2018]. Contour-based Frequency-domain Event Detection for Seismic Arrays, *Seismological Research Letters, **89***: 1514-1523, doi: 10.1785/0220170242 2018.

Rollins, C., R. S. Stein, G. Lin and D. Kilb [2019]. The Ridgecrest earthquakes: Torn ground, nested foreshocks, Garlock shocks, and Temblor's forecast. *Temblor*, http://doi.org/10.32858/temblor.039.

Sahakian*** V., A. Baltay, T. Hanks, J. Buehler***, F. Vernon and D. Kilb [2018]. Decomposing leftovers: Event, path, and site residuals for a small-magnitude ANZA region GMPE, *Bull. Seism. Soc. Am.*, ***108***: 2478-2492. https://doi.org/10.1785/0120170376.

Sahakian***, V. J., A. Baltay, T.C. Hanks, J. Buehler***, F.L. Vernon, D. Kilb and N.A. Abrahamson [2019]. Ground motion residuals, path effects, and crustal properties: A pilot study in Southern California. *Journal of Geophysical Research: Solid Earth, **124***(6), 5738-5753. doi: 10.1029/2018jb016796.

* graduate student ** high school intern *** post-doc

GABI LASKE
Professor in Residence

glaske@ucsd.edu, 858-534-8774

Regional and global seismology; surface waves and free oscillations; seismology on the ocean floor; observation and causes of seismic noise; natural disasters and the environment

Gabi Laske's main research area is the analysis of seismic surface waves and free oscillations, and the assembly of global and regional seismic models. She has gone to sea to collect seismic data on the ocean floor. Laske's global surface wave database has provided key upper mantle information in the quest to define whole mantle structure. Graduate students Christine Houser and Zhitu Ma as well as students from other universities have used her data to assemble improved mantle models.

Global reference models: Laske continues collaboration with Guy Masters to compile and distribute global crustal models. CRUST1.0, A 1-degree crustal model, was released in 2013. Applications relying on CRUST1.0 are found across multiple disciplines in academia and industry. Laske maintains the distribution website and provides guidance to users. A new collaboration with colleagues at Christian-Albrecht University of Kiel, Germany focuses on the crust and uppermost mantle in the Mediterranean Sea. The AnICEotropy project: Laske has been collaborating with Fabian Walter and his graduate student Fabian Lindner at ETH, Switzerland to study ice quakes on the Glacier de la Plaine Morte, Switzerland (Figure 22). This plateau glacier that separates Cantons Berne and Valais develops a glacier lake, Lac des Faverges, during snow melt that frequently drains and floods the Simme valley to the north. Recent floods have become more frequent and larger, approaching the capacity of the flood control system. In 2016, Laske, her student Adrian Doran, and collaborators conducted an field experiment to identify precursory ice quake activity that helps improve early flood warning (publication in press). This deployment also allowed a 'sandbox' azimuthal anisotropy analysis to test the hypothesis that seismic anisotropy is aligned with the crevasses on the glacier. Laske was the lead mentor for Fabian Lindner in the analysis of azimuthal anisotropy. She and student Adrian Doran took over modeling for anisotropy with depth (Figure 23). This work is published.

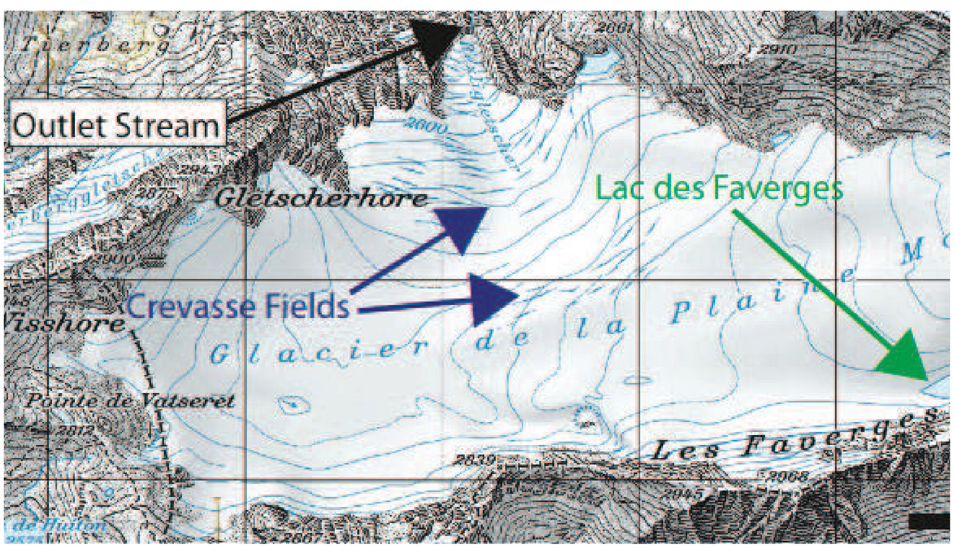

Figure 22. Map of Glacier de la Plaine Morte just south of Wildstrubel, Switzerland. The Rhone valley is to the south. Marked is the outlet stream at the toe of Rexliglacier that drains into the Simme river to the north. Arrows mark Lac des Faverges, a major glacier lake, and the two crevasse fields that Laske and Walter occupied with four seismic arrays (purple stars) during summer 2016. The instruments were borrowed from the GIPP instrument pool at GFZ, Potsdam, Germany.

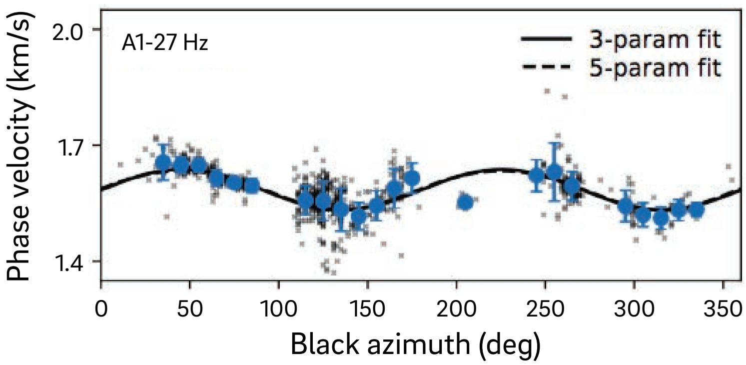

Figure 23. Measured azimuthal anisotropy at 27 Hz at array A1. Azimuthal anisotropy is modeled by a truncated trigonometric polynomial of degrees 2 and 4 in back azimuth. A decline of arimuthal anisotropy with decreasing frequency (not shown) indicates a shallow (20-30 m) origin for the anisotropy.

The PLUME project: For the past decade or so, Laske has analyzed waveforms collected on ocean bottom seismometers (OBSs). She was the lead-PI of the Hawaiian PLUME project (Plume–Lithosphere–Undersea–Mantle Experiment) to study the plumbing system of the Hawaiian hotspot. Results from various body wave, surface wave and receiver function studies were published. Most recently, PhD student Adrian Doran studied seafloor compliance and ambient-noise Green's functions. His most recent paper describes a Monte-Carlo search for sediment and uppermost crustal structure using seafloor compliance and well as converted phases from the sediments. In the meantime, Laske received funding to conduct a similar OBS experiment in 2021 halfway between Hawaii and North America to investigate 40-50 Myr old northeast Pacific lithosphere.

The CABOOSE project: The CAlifornia BOrderland Ocean SEismicity project (CABOOSE) is a collection of small OBS deployments, past and on-going, to assess seismicity off-shore Southern California. In 2014, a 3-month deployment about 300 km west of La Jolla revealed never-before seen seismic activity in the Outer Borderland. Doran and Laske returned in the summers of 2015, 2017 and 2018 on UC ship fund cruises to continue investigation of the inner Borderland seismicity in more detail. We currently analyze data collected on the San Clemente Fault. The rich dataset reveals numerous repeat events that have not been detected by the Southern California Seismic Network. For this deployment, development engineer Martin Rapa designed an in-situ calibration frame for the pressure sensor to help better understand the still poorly known instrument response of that sensor. Graduate student Adrian Doran and Laske successfully modeled the time series collected for a defined 3-inch drop and benchmarked their results against more traditional calibration efforts using earthquake and Earth tide data.

RECENT PUBLICATIONS

Laske, G., El-Sharkawy, A. and Meier, T., Crustal Model Validation in the Mediterranean Sea. *Geophys. Res. Abstr.,* ***21,*** EGU20189-2644, 2019.

Doran, A.K. and Laske, G., Seismic structure of marine sediments and upper oceanic crust surrounding Hawaii. *J. Geophys. Res.,* ***124,*** 2038–2056, doi: 10.1029/2018jb016548, 2019.

Doran, A.K., Rapa, M., Laske, G., Babcock, J. and McPeak, S., Calibration of differential pressure gauges through *in situ* testing. *Earth Space Sci.,* in press, 2019.

Lindner, F., Laske, G., Walter, F. and Doran, A.K., Crevasse-induced Rayleigh-wave azimuthal anisotropy on Glacier de la Plaine Morte, Switzerland. *Annals of Glaciology,* doi: 10.1017/aog.2018.25, 2018.

Lindner, F., Walter, F. Laske, G., and Gimbert, F. Glaciohydraulic seismic tremors on an Alpine glacier. *The Cryosphere,* in press, 2019.

MATTHIAS MORZFELD
Associate Professor

matti@ucsd.edu, igppweb.ucsd.edu/~mmorzfeld

Computational & stochastic modeling, sampling methods for inverse problems, numerical analysis, reduced order modeling

The common theme that ties my work together is merging computational models with data via a Bayesian approach. This is easy to explain with the example of a weather forecast, but the general approach is used throughout the Earth sciences (see below for recent examples). Suppose you use a mathematical model for the weather to make a weather forecast. If the model calls for rain but you wake up to sunshine, then you should calibrate your model to this observation before you make a forecast for the next day. This is an example of Bayesian inference. My research focuses on the design, analysis and application of numerical methods for this problem.

Over the past year, the algorithms and mathematical techniques I work on have been used in a variety of fields in Earth science and engineering. Examples include the computational modeling of pre-mixed flames, the modeling of the Earth's magnetic dipole field over millions of years, new models for cloud microphysics, and intra-hour forecasts of the cloud index for the greater Tucson, AZ, area. The latter is particularly useful for managing the power grid in view of an increasing amount of renewable energy being fed into the grid.

I have also studied in depths some more theoretical and mathematical aspects of Bayesian inverse problems. One issue that stands in the way of the wide application of modern techniques for solving inverse problems is the extreme dimensionality that is typical of problems in Earth science. For example, a computational model for the Earth's magnetic field has more than tens of millions of unknown variables. By studying analogies of sampling methods and well-known solvers in linear algebra, my collaborators and I could make significant progress in understanding how solving inverse problems in extreme dimensions can function. Another mathematical project revolves around how the high complexity and fidelity of new computational models necessitates using new numerical methods for inverse problems.

RECENT PUBLICATIONS

M. Van Lier-Walqui, H.C. Morrison, M.R. Kumjian, K.J. Karly, J. Reimel, O.P. Prat, S. Lunderman and M. Morzfeld, A Bayesian approach for statistical-physical bulk parameterization of rain microphysics, Part II: Idealized Markov chain Monte Carlo experiments, Journal of the Atmospheric Sciences, accepted for publication.

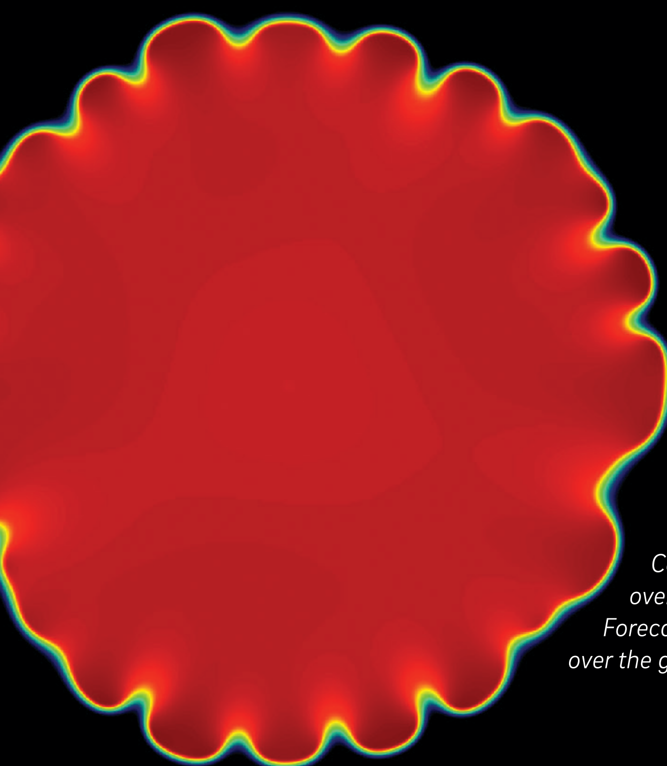

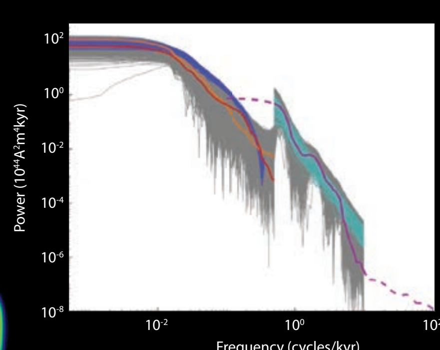

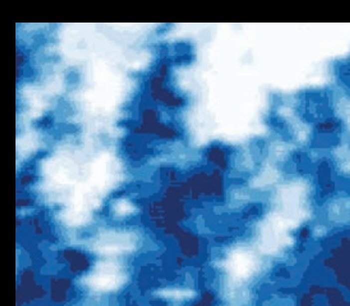

Figure 24. Three very different Bayesian estimation problems with a very similar mathematical formulation. Left: Sample of a high-fidelity simulation of a pre-mixed flame, calibrated to data from 91 experiments. These calculations were performed on the Department of Energy's super computers. Center: mathematical model for the variations of Earth's magnetic dipole field over millions of years and comparison to paleomagnetic observations. Right: Forecast of the "cloud index" (related to how much sunlight can hit a solar cell array) over the greater Tucson, AZ, area for a day in April.

M. Morzfeld and D. Hodyss, Gaussian approximations in filters and smoothers for data assimilation, Tellus A: Dynamic Meteorology and Oceanography, 71:1, 1-27 (2019).

M. Morzfeld, X.T. Tong and Y.M. Marzouk, Localization for MCMC: sampling high-dimensional posterior distributions with local structure, Journal of Computational Physics, 380, 1–28 (2019).

M. Morzfeld and B.A. Buffett, A comprehensive model for the kyr and Myr time scales of Earth's axial magnetic dipole field, Nonlinear Processes in Geophysics, 26, 123-142 (2019).

J.B. Bell, M.S. Day, J. Goodman, R.W. Grout and M. Morzfeld, A Bayesian approach to calibrating hydrogen flame kinetics using many experiments and parameters, Combustion and Flame 205, 305–315 (2019).

T.M. Harty, W.F. Holmgren, A.T. Lorenzo, M. Morzfeld, Intra-hour cloud index forecasting with data assimilation, Solar Energy 185, 270-282 (2019).

ROSS PARNELL-TURNER

Assistant Professor

rparnellturner@ucsd.edu, 858-822-2975

Melting and deformation on mid-ocean ridges, mantle dynamics

I'm a marine geophysicist, and my research uses geophysical observations to learn about how oceanic crust is created and deformed, with a focus on slow-spreading ridges, and on plume-ridge dynamics.

Significant portions of seafloor in the North Atlantic ocean are presently forming through asymmetric spreading, which can lead to the development of low-angle faults called oceanic detachments. However, seafloor exposures of corrugated fault surfaces, a telltale sign of detachment fault growth, are often spatially confined (≤10 km along-axis) and only make up a small fraction of the >40 km-long asymmetric sections of slow-spreading ridges. One explanation may be that detachment faults underlie entire ridge segments but are only exposed in areas where hanging wall rider blocks cannot develop. Another is that detachment faults have a limited along-axis extent and connect with shorter-offset faults through complex relay structures With colleagues from France, Germany and the USA, we tackled this problem using near-bottom bathymetric surveys acquired with autonomous underwater vehicles (AUVs) over four corrugated detachments along the Mid-Atlantic Ridge (Parnell-Turner et al., 2018; Olive et al., 2019). We investigated the rafting of hanging

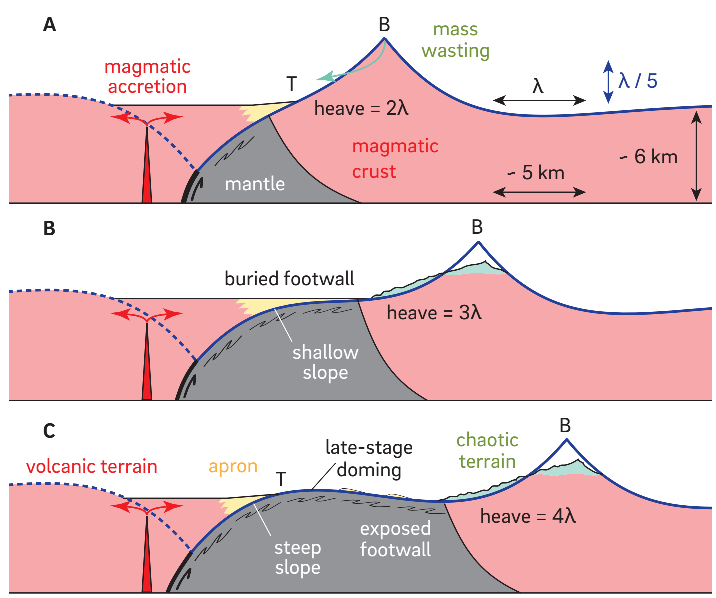

Figure 25. Progressive rollover and exhumation of a detachment fault (Olive et al., 2019). A: At moderate offsets (e.g., fault heave = 2L), footwall slopes are steep, which leads to mass wasting of the breakaway (fc: footwall cutoff) region, eventually forming the chaotic terrain. B: At intermediate offsets (e.g., fault heave = 3L) flexural rotation of the footwall leads to very shallow seafloor slopes, promoting a widespread apron zone burying most of the detachment surface. C: Finally, at large offsets (e.g., fault heave = 4L) late-stage doming occurs close to the fault termination (hc: hanging wall cutoff) where seafloor slopes increase, reducing the extent of the apron and exposing the corrugated detachment surface (wiggly lines).

wall-derived debris over emerging fault scarps, which can lead to covering shallow-dipping corrugated fault surfaces. We modeled this process using critical taper theory, and infer low effective friction coefficients (~0.2) on the shallowest portion of detachment faults. A corollary to this result is that detachments emerging from the seafloor at angles <13° are more likely to become blanketed under an apron of hanging wall material. We generalize these findings as a simple model for the progressive exposure and flexural rotation of detachment footwalls, which accounts for the continued action of seafloor-shaping processes (Figure 25). Our model suggests that many moderate-offset, hidden detachment faults may exist along slow mid-ocean ridges, and do not feature an exposed fault surface.

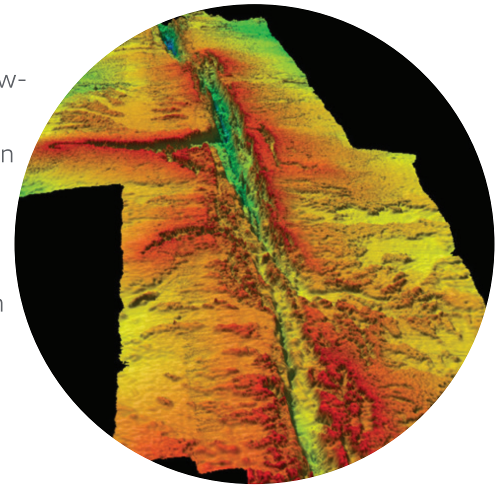

Figure 26. 3-D perspective view of 1 m resolution multibeam bathymetric data collected by Sentry in December 2018 over the axial summit trough at 9°50′N, looking north.

The 9°50′N of the East Pacific Rise is known to be one of the most volcanically active regions of the global mid-ocean ridge network. Eruptions in 1991 and 2005 were documented with mapping, submersible dives, sampling, temperature and seismic monitoring, leading to the notion that the magma system is likely to erupt on a ~15 year cycle, and is likely to erupt in the next 2–3 years. In order to quantify the volume and flow dynamics of the next likely eruption, a baseline survey of meter-scale resolution mapping and vent temperature data is required. We conducted a preliminary mapping survey using AUV *Sentry* in December 2018 (Figures 26 and 27), which covered a portion of the anticipated eruption area, with more mapping scheduled in 2019 to complete the effort. Self-contained temperature probes were installed in vent orifices to monitor temperature increases, and we measured temperature and current flow velocity at 20 m above the active vent fields, using instruments mounted on Sentry in order to quantify the heat flow processes within the water column.

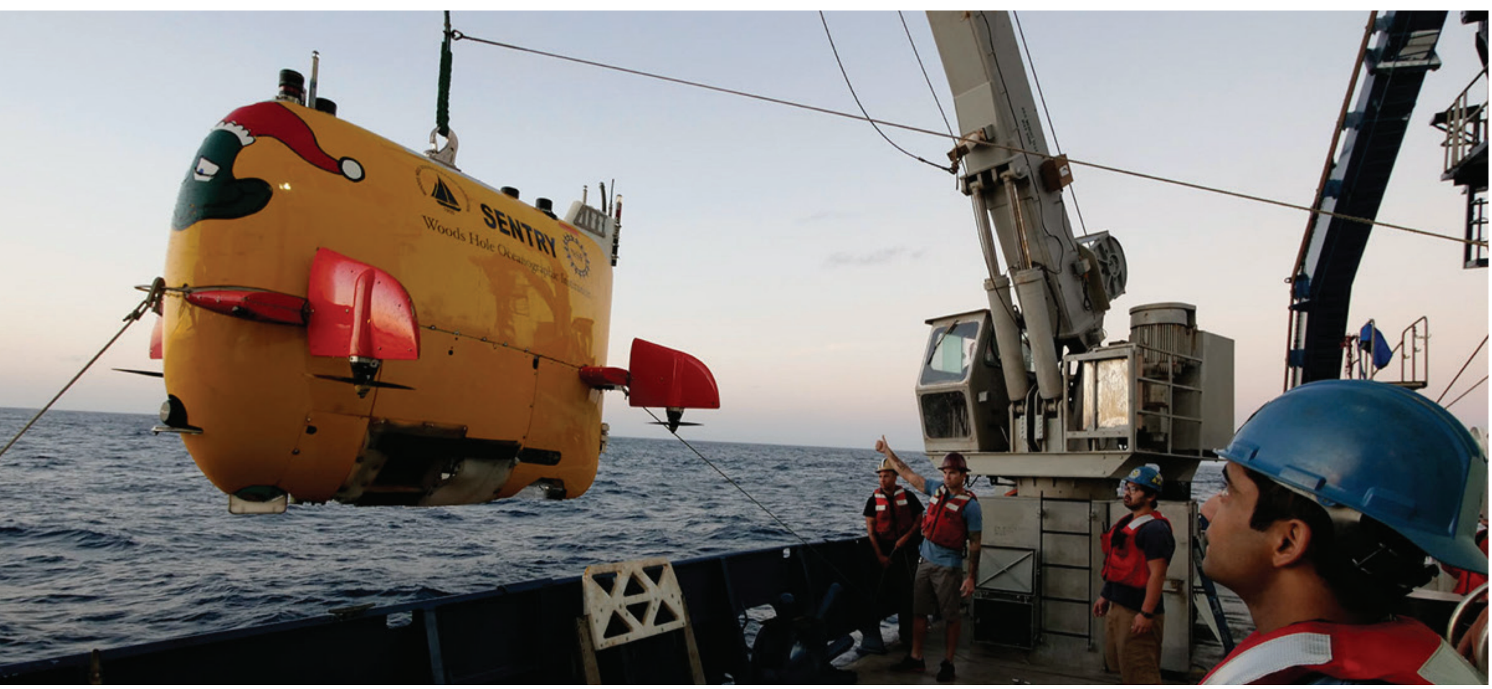

Figure 27. AUV Sentry *being deployed over the side of R/V* Atlantis.

RECENT PUBLICATIONS

Parnell-Turner, R., Escartín, J., Olive, J.A., Smith, D.K., Petersen, S., 2018a. Genesis of corrugated fault surfaces by strain localization recorded at oceanic detachments. *Earth Planet. Sci. Lett.* ***498***, 116–128, doi:10.1016/j.epsl.2018.06.034

Olive, J.-A., R. Parnell-Turner, J. Escartín, D. K. Smith, and S. Petersen (2019), Controls on the Seafloor Exposure of Detachment Fault Surfaces, *Earth Planet. Sci. Lett.* ***506***, 381–387, doi:10.1016/j.epsl.2018.11.001.

ANNE POMMIER
Assistant Professor

pommier@ucsd.edu, 858-822-5025

Physics and chemistry of silicate melts and metal alloys; role of magma in planetary interiors, from the scale of volcanic magma reservoirs to planetary-scale magma oceans; evolution of planetary interiors from "deep time" (e.g., planet evolution) to the present

Over the past 12 months, efforts have been mostly spent on the investigation of (i) Mercury's core, (ii) the fate of water in subduction zones, and (iii) tidal heating in Jupiter's Moon Io. (i) and (ii) were funded by NSF grants, and (iii) is the result of the Tidal Heating Workshop organized by the Keck Institute for Space Studies at Caltech last Fall.

(i) Mercury' weak intrinsic magnetic field is intimately tied to the structure and cooling history of its core. Recent constraints about the planet's internal structure suggest the presence of a FeS layer overlying a silicon-bearing core. Together with K. Leinenweber (ASU) and SIO undergraduate student T. Tran, we performed 4-electrode resistivity experiments on core analogues up to 10 GPa and over wide temperature ranges in order to investigate the insulating properties of core materials (Pommier et al., 2019a). Experiments were performed in the Planetary and Experimental Petrology Laboratory (PEPL) at SIO-IGPP. Our results show that the FeS layer is liquid and insulating compared to the rest of the core, and that the electrical resistivity of a miscible Fe-Si(-S) core is comparable to the one of an immiscible Fe-S, Fe-Si core. The difference in electrical resistivity between the FeS-rich layer and the underlying Fe-Si(-S) core is at least 1 log unit at pressure and temperature conditions relevant to Mercury's interior. Using our electrical results to compute thermal conductivity for FeS and Fe-Si(-S) materials, we suggest that a thick (> 40 km) FeS-rich shell is expected to maintain high temperatures across the core, and if temperature in this layer departs from an adiabat, then this might affect the cooling rate of Mercury's core. The presence of a liquid and insulating shell is not inconsistent with a thermally stratified core in Mercury and could impact the sustainability of the intrinsic magnetic field.

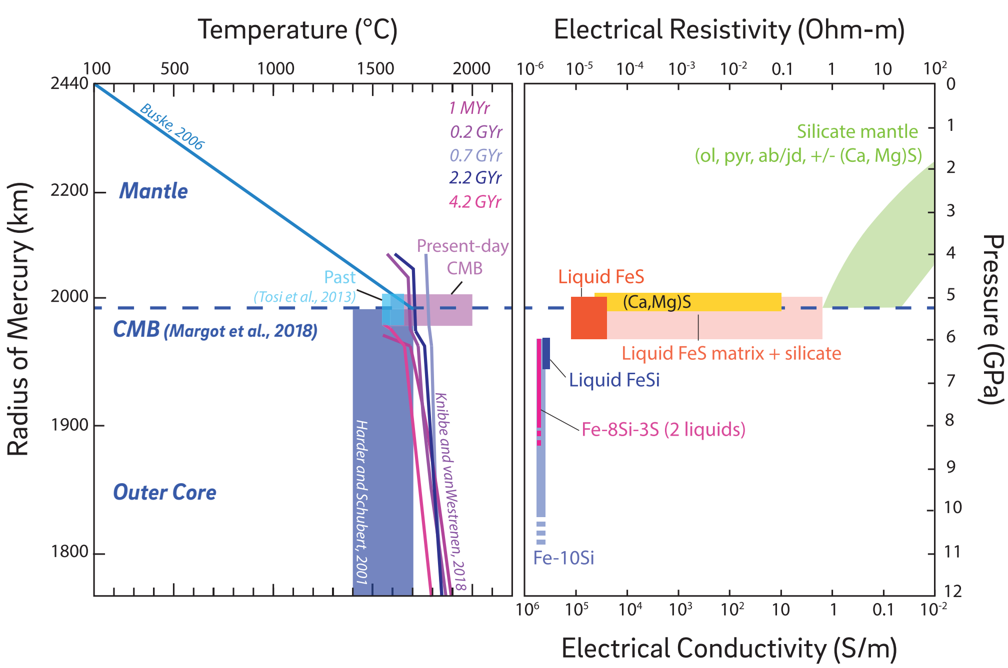

Figure 28. Internal thermal (left) and electrical (right) structure of Mercury's mantle and outer core. The depth of the core-mantle boundary (CMB) is from Margot et al. (2018). Thermal structure for the present-day and past comes from Harder and Schubert (2001), Buske (2006), Tosi et al. (2013), and Knibbe and van Westrenen (2018). In these models, Mercury's core heats up in the first 2 Ga. Electrical resistivity for different compositions investigated in this study is presented and indicate an insulating outermost core. Mantle resistivity (green) is calculated using the geometric means (Pommier et al., EPSL, 2019).

(ii) Silicate mineral lawsonite ($CaAl_2Si_2O_7(OH)_2 \cdot H_2O$) represents a particularly efficient water reservoir in subduction contexts, as it can carry about 12 wt % water at depth and is stable in the slab over a wide pressure range. In collaboration with Q. Williams (UCSC) and R.L. Evans (WHOI), we measured the electrical properties of natural polycrystalline lawsonite from 300 to about 1325 °C and up to 10 GPa using the multi-anvil apparatus in PEPL (Pommier et al., 2019b). We observe that temperature increases lawsonite conductivity until fluids escape the cell after dehydration occurs. We suggest that lawsonite dehydration could contribute to (but not solely explain) high conductivity anomalies observed in the Cascades by releasing aqueous fluid at a depth (~50 km) consistent with the basalt-eclogite transition. In subduction settings where the incoming plate is older and cooler (e.g., Japan), lawsonite remains stable to great depth. In these cooler settings, lawsonite could represent a vehicle for deep water transport and the subsequent triggering of melt that would appear electrically conductive, though it is difficult to uniquely identify the contributions from lawsonite on field electrical profiles in these more deep-seated domains.

(iii) The evolution of the state of a terrestrial body over geologic time requires understanding material properties that are constrained by laboratory data. A very exciting and emerging research direction focuses on the study of tidal heating. Io is an ideal candidate to study tidal heating because of the effect of Jupiter's tidal forcing on its interior. Since 10/2018 and following an invitation to attend a Keck workshop in Caltech (de Kleer et al., 2019), I am a co-PI on the science team of NASA's Io Volcano Observer mission concept led by Alfred McEwen (U of A). We identified five key questions to drive future research and exploration: What do volcanic eruptions tell us about the interiors of tidally heated bodies? How is tidal dissipation partitioned between solid and liquid materials? Does Io have a melt-rich layer, or "magma ocean", that mechanically decouples the lithosphere from the deeper interior? Is the Jupiter/Laplace system in equilibrium (i.e., does the satellite's heat output equal the rate at which energy is generated)? Can stable isotope measurements inform long-term evolution of tidally heated bodies?

RECENT PUBLICATIONS

Pommier A., K. Leinenweber, T. Tran, Mercury's Thermal Evolution Controlled by an Insulating Liquid Outermost Core?, *Earth and Planetary Science Letters*, ***517,*** 125-134, 2019.

Pommier A., Q. Williams, R. L. Evans, I. Pal, Z. Zhang, Electrical Investigation of Natural Lawsonite under Temperature in the Pressure Range 1-10 GPa and Application to Subduction Contexts, *J. Geophys. Res.,* 10.1029/2018JB016899, 2019.

de Kleer, K. and the IVO Team, Tidal Heating: Lessons from Io and the Jovian System, Final Report for the Keck Institute for Space Studies, 2019 (https://kiss.caltech.edu/final_reports/Tidal_Heating_final_report.pdf).

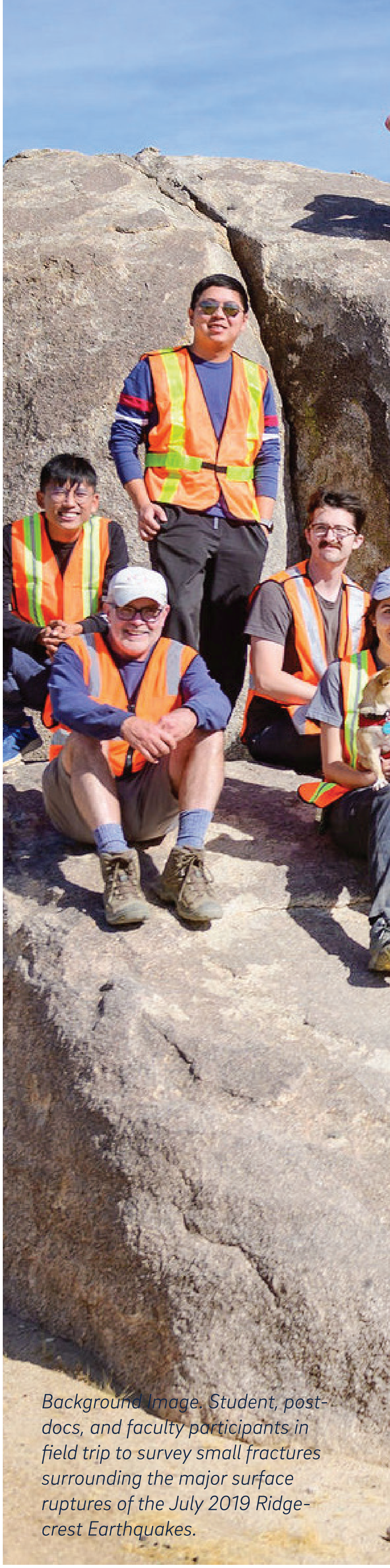

Background Image. Student, post-docs, and faculty participants in field trip to survey small fractures surrounding the major surface ruptures of the July 2019 Ridgecrest Earthquakes.

DAVID T. SANDWELL

Professor of Geophysics

dsandwell@ucsd.edu, http://topex.ucsd.edu

Geodynamics, global marine gravity, crustal motion modeling, space geodesy

Students and Funding: Research for the 2018-19 academic year was focused on understanding the geodynamics of the crust and lithosphere. Our group comprises three graduate students John DeSanto, Hugh Harper, Yao Yu and an undergraduate lab assistant Zhen Yu. We support two postdocs Eric Xu and Brook Tozer. Our research on improvement the marine gravity field is co-funded by NASA and the Office of Naval Research. Our research on strain rate and moment accumulation rate along the San Andreas Fault System from InSAR and GPS is funded by the NASA Earth Surface and Interior Program as well as the Southern California Earthquake Center. We also receive funding from the National Science Foundation to improve the GMTSAR InSAR processing code and documentation (http://topex.ucsd.edu/gmtsar).

Global Gravity and Bathymetry: We are improving the accuracy and spatial resolution of the marine gravity field using data from 5 satellite radar altimeters (CryoSat-2, AltiKa, Jason-2 and Sentinel-3A/B). This is resulting in steasy improvements in the global marine gravity field. Most of the improvement is in the 12 to 40 km wavelength band, which is of interest for investigation of seafloor structures. The improved marine gravity is important for exploring unknown tectonics in the deep oceans as well as revealing thousands of uncharted seamounts (http://topex.ucsd.edu/grav_outreach).

Integration of Radar Interferometry and GPS - We are developing methods to combine the high accuracy of point GPS time series with the high spatial resolution from radar interferometry to measure interseismic velocity along the San Andreas Fault system associated with earthquake hazard (http://topex.ucsd.edu/insargen). Over the past five years, three new InSAR satellites became operational. Sentinel 1A and 1B are the first of a series of European Space Agency (ESA) SAR satellites to provide an operational mapping program for crustal deformation along all zones having high tectonic strain. The third new satellite is ALOS-2, launched by JAXA. These satellites have the measurement cadence and spatial coverage needed to revolutionize our understanding of earthquake cycle processes both globally and along the San Andreas Fault System. A Major earthquake (M7.1) struck Ridgecrest California in July 2019 and the surface deformation was extremely well imaged by these satellites (http://topex.ucsd.edu/SV_7.1/index.html). In addition, we organized two field trips to the area to study small deformations on the many pre-existing faults surrounding the main rupture area (Background Image).

RECENT PUBLICATIONS

Xu, X., D. T. Sandwell, and B. Smith-Konter, Co-seismic Displacements and Surface Fractures from Sentinel-1 InSAR: 2019 Ridgecrest Earthquakes, *Seismological Research Letters,* in press, 2019.

Xu, X., D. T. Sandwell, Toward Absolute Phase Change Recovery With InSAR: Correcting for Earth Tides and Phase Unwrapping Ambiguities, *IEEE Transactions on Geoscience and Remote Sensing,* in press, 2019.

Sandwell, D. T., Harper, H., Tozer, B., & Smith, W. H. (2019). Gravity Field Recovery from Geodetic Altimeter Missions. *Advances in Space Research*.

DeSanto, J. B., & Sandwell, D. T. (2019). Meter-scale seafloor geodetic measurements obtained from repeated multibeam sidescan surveys. *Marine Geodesy*, (just-accepted), 1-10.

DeSanto, J. B., Chadwell, C. D., & Sandwell, D. T. (2019). Kinematic Post-processing of Ship Navigation Data Using Precise Point Positioning. *The Journal of Navigation, **72***(3), 795-804.

Tozer, B., Sandwell, D. T., Smith, W. H. F., Olson, C., Beale, J. R., & Wessel, P. (2019). Global bathymetry and topography at 15 arc seconds: SRTM15+. *Earth and Space Science.*

Klein, E., Bock, Y., Xu, X., Sandwell, D. T., Golriz, D., Fang, P., & Su, L. (2019). Transient deformation in California from two decades of GPS displacements: Implications for a three-dimensional kinematic reference frame. *Journal of Geophysical Research: Solid Earth.*

Xu, X., Ward, L. A., Jiang, J., Smith-Konter, B., Tymofyeyeva, E., Lindsey, E. O., ... & Sandwell, D. T. (2018). Surface creep rate of the Southern San Andreas Fault modulated by stress perturbations from nearby large events. *Geophysical Res. Lett.,* 45(19), 10-259.

PETER SHEARER

Distinguished Professor

pshearer@ucsd.edu, 858-534-2260

Seismology, Earth structure, earthquake physics

My research uses seismology to learn about Earth structure and earthquakes, using data from the global seismic networks and local networks in California, Nevada, Hawaii, and Japan. My work in crustal seismology has focused on improving earthquake locations using waveform cross-correlation, systematically estimating small-earthquake stress drops from P-wave spectra, and studying properties of earthquake clustering, especially swarms and foreshock sequences. At deeper depths, much of my research has involved resolving properties of the mantle transition-zone discontinuities.

Former graduate student and postdoc Janine Buehler analyzed data from the USArray seismic experiment and developed a new method to image upper-mantle discontinuities using top-side reflections of long-period S-waves from distant earthquakes. We observe clear reflections off the 410- and 660-km discontinuities (see Figure 1), which can be used to map the depth and brightness of these features. Because our results are sensitive to the impedance contrast (velocity and density), they provide a useful complement to receiver-function studies, which are primarily sensitive to the S velocity jump alone. Our images show strong discontinuities near 410 and 660 km across the entire USArray

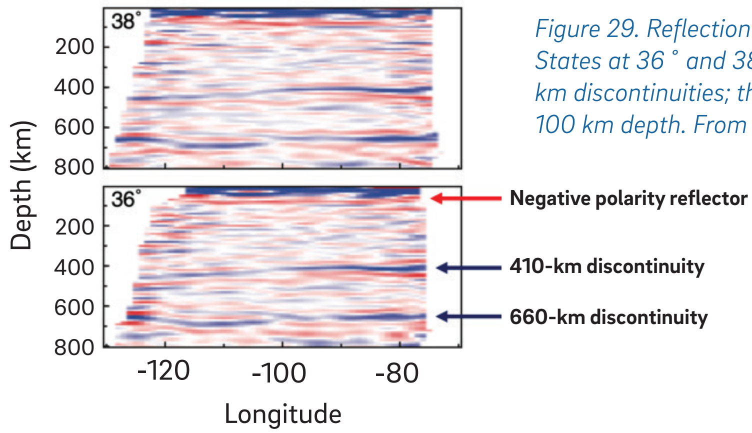

Figure 29. Reflection seismic profiles of the upper mantle under the United States at 36 ° and 38 ° latitude. The blue streaks show the 410- and 660-km discontinuities; the red streak is a negative polarity reflector (NPR) near 100 km depth. From Shearer and Buehler (2019).

footprint, with intriguing reflectors at shallower depths in many regions. Overall, the discontinuities in the east appear relatively simple with a uniform transition zone thickness of ~250 km. The western US has more complex discontinuity topography, with small-scale changes below the Great Basin and the Rocky Mountains, and a decrease in transition-zone thickness along the western coast. We also observe a negative polarity reflector (NPR) near 100-km depth under much of the US, which is likely the lithosphere-asthenosphere boundary (LAB) in the tectonically active west but whose origins are somewhat mysterious under the stable continental regions of the eastern US.

Vera Schulte-Pelkum (2001 IGPP PhD) recently led a novel project to resolve a long-standing issue—whether deep earthquakes observed under southern Tibet are confined to the thickened crust under the Himalayan collision zone or whether some of them extend into the upper mantle. By comparing earthquake depths resolved using S – P times to Moho depths resolved using receiver functions, she was able to cancel out any uncertainties associated with the seismic velocity structure and prove that some of the seismicity is located below the crust. This result argues against the crustal eclogitization hypothesis to explain the deep seismicity, instead suggesting that other embrittlement mechanisms are operating in the deep mantle.

My research in southern California has continued to focus on improving earthquake locations (e.g., Ross et al., 2019), analyzing spectra to resolve corner frequency and estimate stress drop for small earthquakes (e.g., Shearer et al., 2019), and using coda waves to study scattering and intrinsic attenuation, as well as earthquake source properties (e.g., Wang and Shearer, 2019).

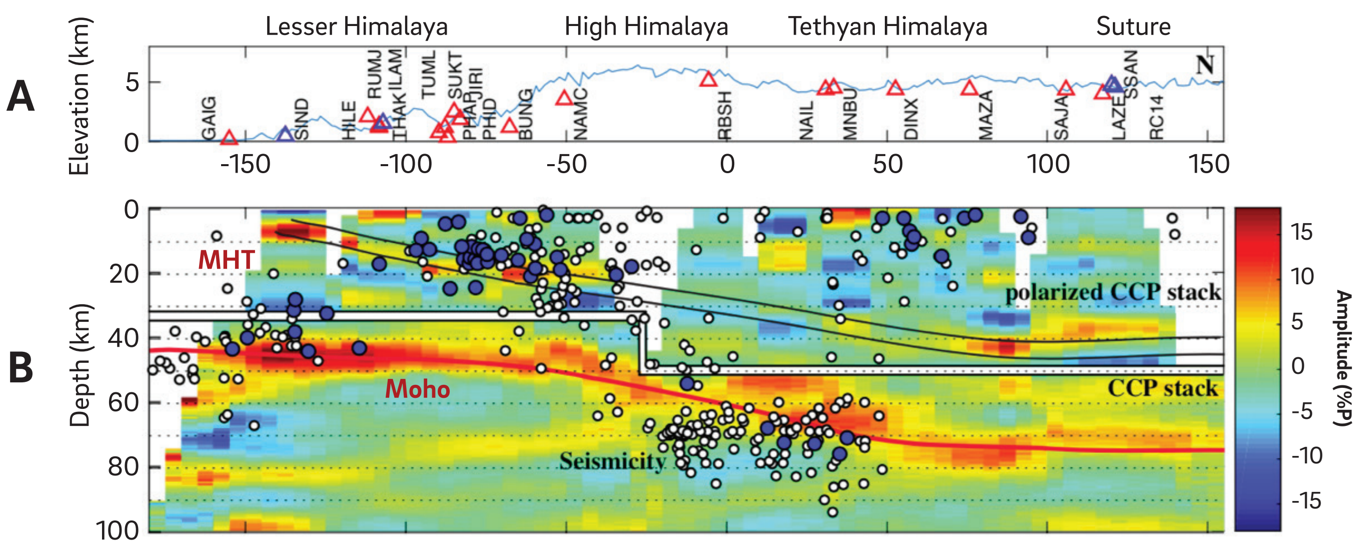

Figure 30. Depth profile across the Himalayas, showing seismic stations (triangles), Moho imaged with receiver functions (red line), and earthquake locations (circles, blue for those located with S – P times). Note the cluster of earthquakes in the upper mantle below the Moho. From Schulte-Pelkum et al. (2019).

RECENT PUBLICATIONS

Wang, W., and P. M. Shearer, An improved method to determine coda-Q, earthquake magnitude and site amplification: Theory and application to southern California, *J. Geophys. Res.,* ***124***, 578-598, doi: 10.1029/2018JB015961, 2019.

Shearer, P. M., R. E. Abercrombie, D. T. Trugman, and W. Wang, Comparing EGF methods for estimating corner frequency and stress drop from P-wave spectra, *J. Geophys. Res.,* ***124***, 3966-3986, doi: 10.1029/2018JB016957, 2019.

Ross, Z. E., D. T. Trugman, E. Hauksson, and P. M. Shearer, Searching for hidden earthquakes in Southern California, *Science,* ***364***, 767-771, 10.1126/science.aaw6888, 2019.

Schulte-Pelkum, V., G. Monsalve, A. F. Sheehan, P. Shearer, F. Wu, and S. Rajaure, Mantle earthquakes in the Himalayan collision zone, *Geology,* https://doi.org/10.1130/G46378.1, 2019.

Shearer, P. M., Introduction to Seismology, Third Edition, Cambridge University Press, IBSN: 9781316635742, Cambridge, 2019.

Shearer, P. M., and J. Buehler, Imaging upper-mantle structure under USArray using long-period reflection seismology, *J. Geophys. Res.*, doi: 10.1029/2019JB017326, 2019.

Shearer, P. M., SSA Presidential Address, in 2019 SSA Annual Meeting Report, *Seismol. Res. Lett.,* ***90***, 2063-2064, 2019.

LEONARD J. SRNKA

Professor of Practice

lsrnka@ucsd.edu, 858-822-1510

Land and marine electromagnetic (EM) methods; integrated geophysical data analysis and interpretation; inverse theory; energy outlooks and global change

A key aspect of subsurface imaging is quantifying the spatial resolution and uncertainties in extracted parameters obtained from various probing methods; i.e. what can be deduced from the results, and with what confidence? This is known as the inference problem, important to both academic and applied studies. A well-known example is found in controlled source reflection seismology, which is the mainstay of the natural resource industry. Perhaps the last remaining "grand challenge" for geophysical electromagnetic (EM) methods is the equivalent quantification of resolution and uncertainty in EM imaging techniques. Most of these techniques use nonlinear mathematical inversions, in which making inference is a daunting task. Approaches include theoretical-analytical methods (Medin et al., 2007; Constable et al., 2017), deterministic (Gist et al., 2013), and various statistical methods (Chen et al., 2012; Ray and Key, 2012; Ray et al., 2013, 2014; Houck et al., 2013). EM detection and resolution of subsurface features are directly (but not linearly) dependent on the accuracy of phase and amplitude measurements in the presence of noise. But since these are always inexact, the derived answers are always non-unique.

It may be that the best possible formal results can determine only average values and uncertainties within a chosen depth range (R.L. Parker, SEMC Workshop, La Jolla 2017 and private communication, 2019). Medin et al. (2007) show a good example of this for the case of 1D (i.e. spherically symmetric) geomagnetic sounding.

The lack of practical EM inference methods, even if these are ad hoc but still useful (e.g. not quite theoretically correct), is probably the single biggest obstacle to better acceptance and more uptake of EM methods. One approach to EM inference that has been explored rather lightly is whether analogies from the propagational wave (e.g. seismic) case can be used to make progress on the diffusive wave EM case. Current understanding would lead us to say no – the physics are just too different. L. Thomsen (2014) discussed the differences and similarities in some detail, and argues that EM data can be imaged in a manner analogous to very attenuative reflection seismic data, and that an impulsive-type source is preferred over continuous waveforms. As examples of EM differences, vertical and lateral resolution are usually different for resistive and conductive targets, for different source types (e.g. controlled-source EM (CSEM) and natural-source methods such as magnetotellurics (MT)), and sometimes for various EM field components specific to the imaging problem. Nevertheless, research has begun in IGPP on exploring semi-correct EM inference methods, starting with literature searches and polling the EM community. Discussions at technical conferences and consortium meetings such as the Scripps Seafloor Electromagnetic Methods Consortium (SEMC) are proving to be fruitful.

For example, experience-based rules of thumb are sometimes used, based partly on the physics of EM diffusive propagation but also on learning from modeling and inversion experiments and from field data. The applicability of such ad hoc rules varies with data type and quality, and also on the geologic situation. Such rules may provide useful guidance on resolution and parameter estimation, but credibility in their validity ranges from "none" to "maybe". Responses from the EM community over the past year have included the following potpourri of ad hoc rules: vertical resolution is inversely proportional to depth; vertical resolution is X percent of the depth (X=10, 20, 30, ….), depending on the source bandwidth; lateral resolution (e.g. edge detection) is comparable to vertical resolution; lateral resolution is proportional to receiver spacing; at least one lateral dimension of a subsurface resistor needs to be comparable to or greater than its depth in order to be detectable; effective depth of investigation is 1/X times the acquisition aperture (X=1, 2, 3,..; effective depth of investigation is X plane-wave skin depths at the lowest source frequency (X=1, 1.5, 2,…); effective depth of investigation can be estimated by placing a highly conductive half-space/full-space at the bottom of the starting model, and then gradually decreasing its depth until the inversion no longer adequately fits the data (an R. L. Parker suggestion); resistivity is always underestimated in inversions; and, spatial resolution and resistivity accuracy depend on the inversion method used. Codification of these seems warranted.

Research in progress is investigating these and other approximate inference methods, starting with single-frequency model data pseudosections and inversions. One interesting avenue of work evaluating the applicability of seismic vibrator reflection data processing, in which the measured source signal is deconvolved from the recorded data at each receiver location, but modified for the strongly dissipative behavior of diffusive (anomalously dispersive) EM propagation where there is no well-defined group velocity. In its place, the center-of-energy velocity, discussed many years ago by Vainshtein (1957) and Brillouin (1960), and more recently by Mainardi (1983), may prove to be a useful (if not exactly correct) substitute.

RECENT PUBLICATIONS

Vainshtein, L. A., 1957. Group velocity of damped waves. *Soviet Phys. Techn. Phys.,* ***2,*** 2420-2428.

Brillouin, L. A., 1960. Wave Propagation and Group Velocity, Academic Press, New York.

Mainardi, F., 1983. Signal velocity for transient waves in linear dissipative media. *Wave Motion* ***5,*** 33-41.

Medin, A. E., R. L. Parker and S. Constable, 2007. Making sound inferences from geomagnetic sounding. *Phys. Earth Planet. Int.,* ***160,*** 51–59.

Chen, J., G. Hoversten, K. Key, G. Nordquist, and W. Cumming, 2012. Stochastic inversion of magnetotelluric data using sharp boundary parameterization and application to a geothermal site. *Geophysics,* ***77,*** E265–E279, doi:10.1190/GEO2011-0430.1.

Ray, A. and K. Key, 2012. Bayesian inversion of marine CSEM data with a trans-dimensional self-parametrizing algorithm. *Geophysical Journal International,* ***191,*** 1135–1151.

Ray, A., D. Alumbaugh, G.M. Hoversten, and K. Key, 2013. Robust and accelerated Bayesian inversion of marine controlled-source electromagnetic data using parallel tempering. *Geophysics,* ***78,*** E271—E280.

Ray, A., K. Key, T. Bodin, D. Myer, and S. Constable, 2014. Bayesian inversion of marine CSEM data from the Scarborough gas field using a transdimensional 2-D parameterization. *Geophysical Journal International,* ***199,*** 1847–1860, doi: 10.1093/gji/ggu370.

Constable, S., A. Orange, and K. Key, 2015. And the geophysicist replied: "Which model do you want?". *Geophysics,* ***80,*** E197–E212.

Gist, G., A. Ciucivara, R. Houck, M. Rainwater, D. Willen, and J.-J. Zhou, 2013. Case Study of a CSEM False Positive - Orphan Basin, Canada. Technical Program Extended Abstracts, *SEG Annual Meeting,* 805-808.

Houck, R. T., A. Ciucivara, and S. Hornbostel, 2013. Probabilistic Interpretation of CSEM Resistivity. Extended Abstracts, *SEG Annual Meeting,* 718-721.

Thomsen, L. 2014. Electromagnetics and seismics: the deep connections. Technical Program Extended Abstracts, *SEG Annual Meeting,* 855-859, doi: 10.1190/segam2014-0798.1.

PETER WORCESTER

Researcher Emeritus

pworcester@ucsd.edu, 858-534-4688

Research Interests: Acoustical oceanography, ocean acoustic tomography, underwater acoustics.

My research is focused on the application of acoustic remote sensing techniques to the study of large-scale ocean structure and on improving our understanding of the propagation of sound in the ocean, including the effects of scattering from small-scale oceanographic variability. My recent research has been focused in the Arctic Ocean, which is undergoing dramatic changes in both the ice cover and ocean structure. Changes in sea ice and the water column affect both acoustic propagation and ambient sound. This implies that what was learned about Arctic acoustics in the past is now obsolete. I have most recently been involved in the analysis of data collected during the Canada Basin Acoustic Propagation Experiment (CANAPE) and in the preparations for and deployment of the joint U.S.-Norwegian Coordinated Arctic Acoustic Thermometry Experiment (CAATEX). Here I report on the CANAPE experiment. My colleague, Dr. Matthew Dzieciuch, reports on the CAATEX experiment in his report.

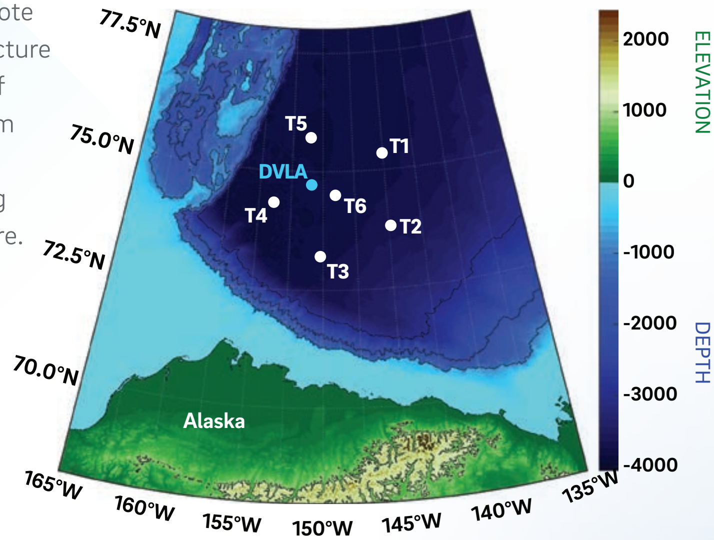

Figure 31. The 2016–2017 CANAPE experiment consisted of six Teledyne Webb Research acoustic transceivers (T1–T6) and a DVLA receiver (DVLA). The array radius is 150 km.

CANAPE was designed to determine the fundamental limits to the use of acoustic methods and signal processing imposed by ice and ocean processes in the new Arctic. To achieve this goal, the CANAPE project conducted two experiments: (1) the short term 2015 CANAPE Pilot Study and (2) the yearlong 2016–2017 CANAPE experiment (Fig. 31). The hope is that these first steps will lead to a permanent acoustic monitoring, navigation, and communications network in the Arctic Ocean. The specific goals of the CANAPE project include (1) understanding the impacts of changing sea ice and oceanographic conditions on acoustic propagation and fluctuations; (2) characterizing the depth dependence and temporal variability of the ambient sound field; and (3) measuring the spatial and temporal variability in the upper ocean throughout the annual cycle by combining acoustic and other data with ocean models.

The 2016–2017 CANAPE experiment included components in both the deep Canada Basin and on the continental shelf and slope north of Alaska. Dr. Dzieciuch and I had primary responsibility for the deep-water CANAPE experiment, for which six acoustic transceiver moorings and a Distributed Vertical Line Array (DVLA) receiver mooring were deployed north of Alaska during August-September 2016 and recovered during September-October 2017 (Fig. 1). The sources transmitted linear frequency-modulated signals with bandwidths of 100 Hz and center frequencies of approximately 250 Hz. The experiment combined measurements of acoustic propagation and ambient sound with the use of an ocean acoustic tomography array to help characterize the oceanographic variability throughout the year in the central Canada Basin. The one-year deployment in a fixed geometry provides measurements in open water during summer, in the marginal ice zone (MIZ) as it transitions across the array during the spring and autumn, and under complete ice cover during winter. All of the ice covering the array during 2016–2017 was first-year ice that reached a maximum thickness of about 1.5 m in late winter and early spring, even though the Canada Basin has historically been a region with extensive multi-year ice that survived over one or more summers.

The measured travel times are remarkably stable, with peak-to-peak variability of only about 20 milliseconds over the entire year. In comparison, travel times in mid-latitudes at similar ranges vary by something like an order of magnitude more (~200 milliseconds peak-to-peak) due to the effects of ocean mesoscale variability with spatial scales of roughly 100 km and time scales of about one month. The high-frequency travel-time fluctuations at periods shorter than a day caused by small-scale oceanographic variability are also much smaller than in mid-latitudes. This was not unexpected, because the ocean internal wave field that scatters sound is much weaker in the Arctic Ocean than in mid-latitudes. In addition, the transmission loss increases significantly in winter, at least in part because of scattering when the signals reflect from the ice cover. Finally, ambient sound also varies over the year, with minimum levels in May-June 2017 when the ice is thickest.

RECENT PUBLICATIONS

Colosi, J. A., B. D. Cornuelle, M. A. Dzieciuch, P. F. Worcester, and T. K. Chandrayadula (2019), Observations of phase and intensity fluctuations for low-frequency, long-range transmissions in the Philippine Sea and comparisons to path-integral theory, *J. Acoust. Soc. Am.,* ***146***(1), 567–585, doi:10.1121/1.5118252.

Howe, B. M., J. Miksis-Olds, E. Rehm, H. Sagen, P. F. Worcester, and G. Haralabus (2019), Observing the oceans acoustically, *Frontiers in Marine Science,* ***6***:426, doi:10.3389/fmars.2019.00426.

Stephen, R. A., S. T. Bolmer, P. F. Worcester, M. A. Dzieciuch, and I. A. Udovydchenkov (2019), Three-dimensional bottom diffraction in the North Pacific, *J. Acoust. Soc. Am.,* ***146***(3), 1913–1922, doi:10.1121/1.5125427.

Worcester, P. F. (2019), Tomography, in Encyclopedia of Ocean Sciences, Third Edition, edited by J. K. Cochran, H. J. Bokuniewicz and P. L. Yager, pp. 328–346, Elsevier, Oxford, doi:10.1016/B978-0-12-409548-9.11591-X.

Cecil H. and Ida M. Green
Institute of Geophysics and Planetary Physics
Scripps Institution of Oceanography, UC San Diego
9500 Gilman Drive, La Jolla, CA 92093-0225, USA
igpp.ucsd.edu